

AIR FORCE INST OF TECH WRIGHT-PATTERSON AFB OH SCHOOL--ETC F/G 22/3
STABILIZING AN UNSTABLE ORBIT ABOUT L3 IN THE SUN, EARTH, MOON --ETC(U)
DEC 79 D E SMITH
AFIT/6A/AA/79D-10 NL

DEC 79 D E SMITH
AFIT/GA/AA/79D-10

NL

UNCLASSIFIED

1 OF 1
AD
012945-61

END
DATE
FILMED
2-80
RDC

ADA 079860



14

AFIT/GA/AA/79D-10

STABILIZING AN UNSTABLE ORBIT ABOUT
 L_3 IN THE SUN, EARTH, MOON SYSTEM
USING LINEAR CONSTANT GAIN FEEDBACK.

9 7/10/80

THESIS

AFIT/GA/AA/79D-10

Doyne E. Smith
Captain USAF

11 1660 77

12 80

DDC
RECEIVED
JAN 23 1980
A

Approved for public release; distribution unlimited

012 225

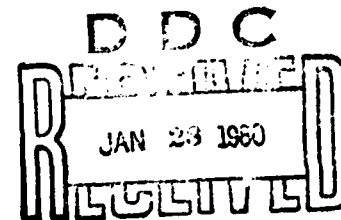
4/5

STABILIZING AN UNSTABLE ORBIT ABOUT
L₃ IN THE SUN, EARTH, MOON SYSTEM
USING LINEAR CONSTANT GAIN FEEDBACK

THESIS

Presented to the Faculty of the School of Engineering
of the Air Force Institute of Technology

Air University (ATC)
in Partial Fulfillment of the
Requirements for the Degree of
Master of Science



by
Doyne E. Smith, B.S.
Captain USAF
Graduate Astronautics
December 1979

Approved for public release; distribution unlimited

Accession For	
NTIS GRA&I	<input checked="checked" type="checkbox"/>
DDC TAB	<input type="checkbox"/>
Unannounced	<input type="checkbox"/>
Justification	<input type="checkbox"/>
By	
Date	
Available for	
Dist	Available for special
A	

Preface

I would like to extend my appreciation to several people for their assistance in this research. First, I would like to express my gratitude to Professor William E. Wiesel for directing me in the choice of subject matter. Further thanks are also due to Professor Wiesel for his advice, encouragement and most of all his understanding during the course of this research. Also, I would like to thank Dr. Robert A. Calico for his time and suggestions which aided immeasurably to my learning experience. Further, I would like to extend a special thanks to my wife for her understanding and inspiration throughout this assignment at the Air Force Institute of Technology. Lastly, her editorial and typing skills were a tremendous asset in completing this document.

Doyne E. Smith

Contents

Preface	ii
List of Figures	iv
List of Symbols	vi
Abstract	viii
I. Introduction	1
Background	1
Problem and Scope	2
II. Problem Analysis	5
Wheeler Model	5
Heppenheimer Model	6
Coordinate Transformation	8
Verification of the Reduced Heppenheimer Equations of Motion	14
III. Feedback Control	24
Stability of Periodic Orbits	24
Feedback Compensation	26
IV. Results and Discussion	50
Results	50
Discussion	52
V. Summary and Recommendations	61
Summary	61
Recommendations	61
Bibliography	63
Appendix A: Derivation of the Heppenheimer Equations of Motion	64
Vita	68

List of Figures

Figure	Page
1 Position of L_3, L_4 and L_5 Orbits with Respect to the Earth and Moon (schematic)	4
2 Wheeler Four-Body Coordinate System	7
3 Heppenheimer Four-Body Coordinate System	9
4 Combined Heppenheimer/Wheeler Coordinate Systems	10
5 L_4 Orbit using the Wheeler Model	18
6 L_4 Orbit using the Reduced Heppenheimer Model	19
7 L_3 Orbit Discovered by Capt Wielsel	20
8 L_3 Orbit using the Reduced Heppenheimer Model	21
9 L_3 Orbit using the Wheeler Model for Four Months	22
10 L_3 Orbit using the Heppenheimer Model for Four Months	23
11 Graph of the "Quasi" Optimization Scheme	28
12 Feedback Control Diagram with Integration Model for Control Cost (schematic)	29
13 "Quasi" Root Locus using Position Feedback (schematic)	31
14 "Quasi" Root Locus using Velocity Feedback (schematic)	32
15 "Quasi" Root Locus using Position/Velocity Feedback (schematic)	33
16 L_3 Orbit using Position Feedback $K_p = 25$ (1 month)	36
17 L_3 Orbit using Position Feedback $K_p = 50$ (1 month)	37
18 L_3 Orbit using Position Feedback $K_p = 100$ (1 month)	38

19	L_3 Orbit using Position Feedback $K_p = 200$ (1 month)	39
20	L_3 Orbit using Position Feedback $K_p = 300$ (1 month)	40
21	L_3 Orbit using Position Feedback $K_p = 400$ (1 month)	41
22	Position Feedback Gain vs Integrated Control Costs	42
23	L_3 Orbit using Velocity Feedback $K_r = 10$ (1 month)	43
24	L_3 Orbit using Velocity Feedback $K_r = 25$ (1 month)	44
25	L_3 Orbit using Velocity Feedback $K_r = 300$ (1 month)	45
26	L_3 Orbit using Position/Velocity Feedback $K_p/K_r = .05$ (1 month) $K_r = 100$	46
27	L_3 Orbit using Position/Velocity Feedback $K_p/K_r = .5$ (1 month) $K_r = 100$	47
28	L_3 Orbit using Position/Velocity Feedback $K_p/K_r = 1$ (1 month) $K_r = 300$	48
29	L_3 Orbit using Position/Velocity Feedback $K_p/K_r = 10$ (1 month) $K_r = 100$	49
30	L_3 Orbit using Position Feedback $K_p = 125$ (2 months)	56
31	L_3 Orbit using Position Feedback $K_p = 400$ (1 month)	57
32	L_3 Orbit using Position/Velocity Feedback $K_p/K_r = 100$ (1 month) $K_r = 1$	58
33	L_3 Orbit using Position/Velocity Feedback $K_p/K_r = 100$ (1 month) $K_r = 10$	59
34	L_3 Orbit using Position/Velocity Feedback $K_p/K_r = 100$ (1 month) $K_r = 100$	60
35	Arbitrary Four-Body System	67

List of Symbols

A	matrix whose components are the partial derivatives of the equations of motion with respect to the states
a	origin of the Wheeler coordinate frame
a_T	total control gain
\hat{a}_1, \hat{a}_2	unit vectors in the Heppenheimer coordinate frame
B_{em}	Earth-Moon barycenter
B_{sem}	Sun-Earth-Moon barycenter
β	angle between the Heppenheimer and Wheeler coordinate frames
b	origin of the Heppenheimer coordinate frame
C_c	total control cost
\hat{e}_1, \hat{e}_2	unit vectors in the Wheeler coordinate frame
\underline{F}_g	Newton's gravitational force
G	gravitational constant
K	constant gain feedback matrix
K_p	position feedback gain factor
K_r	velocity feedback gain factor
L_1-L_5	Lagrange libration points
λ	eigenvalues of Φ
M	mass
μ	mass of the Moon
ω^{ai}	angular rotation rate of the Heppenheimer coordinate frame with respect to inertial space
ω^{ei}	angular rotation rate of the Wheeler coordinate frame with respect to inertial space

Φ	state transition matrix
\underline{r}	position vector with x, y components
σ_j	Poincaré exponents
S_f	time scale factor, Wheeler to Heppenheimer time
t	time
T	integration period
τ_h	Heppenheimer period
τ_w	Wheeler period
$\dot{\theta}$	rotation rate of the Moon about the Earth in the Wheeler coordinate frame
\underline{V}	velocity vector with x, y components
X_c, Y_c	scalar x,y position of the satellite in the Heppenheimer coordinate frame
X_m, Y_m	scalar x,y position of the Moon in the Heppenheimer coordinate frame
X_s, Y_s	scalar x,y position of the Sun in the Heppenheimer coordinate frame
X_α, Y_α	scalar x,y position of the satellite in the Heppenheimer coordinate frame
X_ϵ, Y_ϵ	scalar x,y position of the satellite in the Wheeler coordinate frame
\underline{X}	state vector with components X_1, X_2, X_3, X_4

Abstract

In this study equations of motion for a satellite in a planar, elliptic four-body system are used to generate an orbit about L_3 . Initial conditions and a periodic reference orbit were found using a circular four-body model. Linear constant gain feedback is used to stabilize the orbit about L_3 in the planar, elliptic four-body model. The computed L_3 orbit is plotted against the reference orbit to assess the effectiveness of position, velocity and position/velocity feedback compensation systems. Also computed is the integrated control gain costs for each type of feedback system used. Long term stable motion near libration point L_3 was achieved using position/velocity feedback compensation. Position and velocity feedback when used separately were ineffective as stabilizing feedback compensation systems. The integrated control gain costs also indicate that linear constant gain feedback is not an economical method to stabilize this periodic orbit about L_3 .

STABILIZING AN UNSTABLE ORBIT ABOUT
 L_3 IN THE SUN, EARTH, MOON
SYSTEM USING LINEAR CONSTANT GAIN FEEDBACK

I. Introduction

Background

There is a vast wealth of knowledge on the subject of periodic orbits in the restricted three-body problem. Solutions are well known and show that five equilibrium points exist. They are Lagrange points L_1 , L_2 , L_3 , L_4 and L_5 , so named for the individual who first solved this special case of the restricted three-body problem. Two of the five equilibrium points are stable, namely L_4 and L_5 ; while the remaining three are unstable. Because of the stability properties of L_4 and L_5 , these points have received the greatest amount of numerical analysis over the past twenty years. To a lesser extent the same analysis was performed on L_1 , L_2 and L_3 .

In the restricted four-body problem, stable points L_4 and L_5 do not exist. That is, a satellite placed at L_4 or L_5 , as well as L_1 , L_2 and L_3 , will drift away due to the complex gravitational interaction of the Sun, Moon and Earth. However, with the proper choice of initial conditions, a satellite can have periodic motion about an equilibrium point. This point was covered by Capt. J. E. Wheeler (Ref 1)

in his thesis on periodic motion about L_4 . He found that periodic motion about L_4 did exist in the restricted four-body problem, and that this orbit definitely exhibited linear stability.

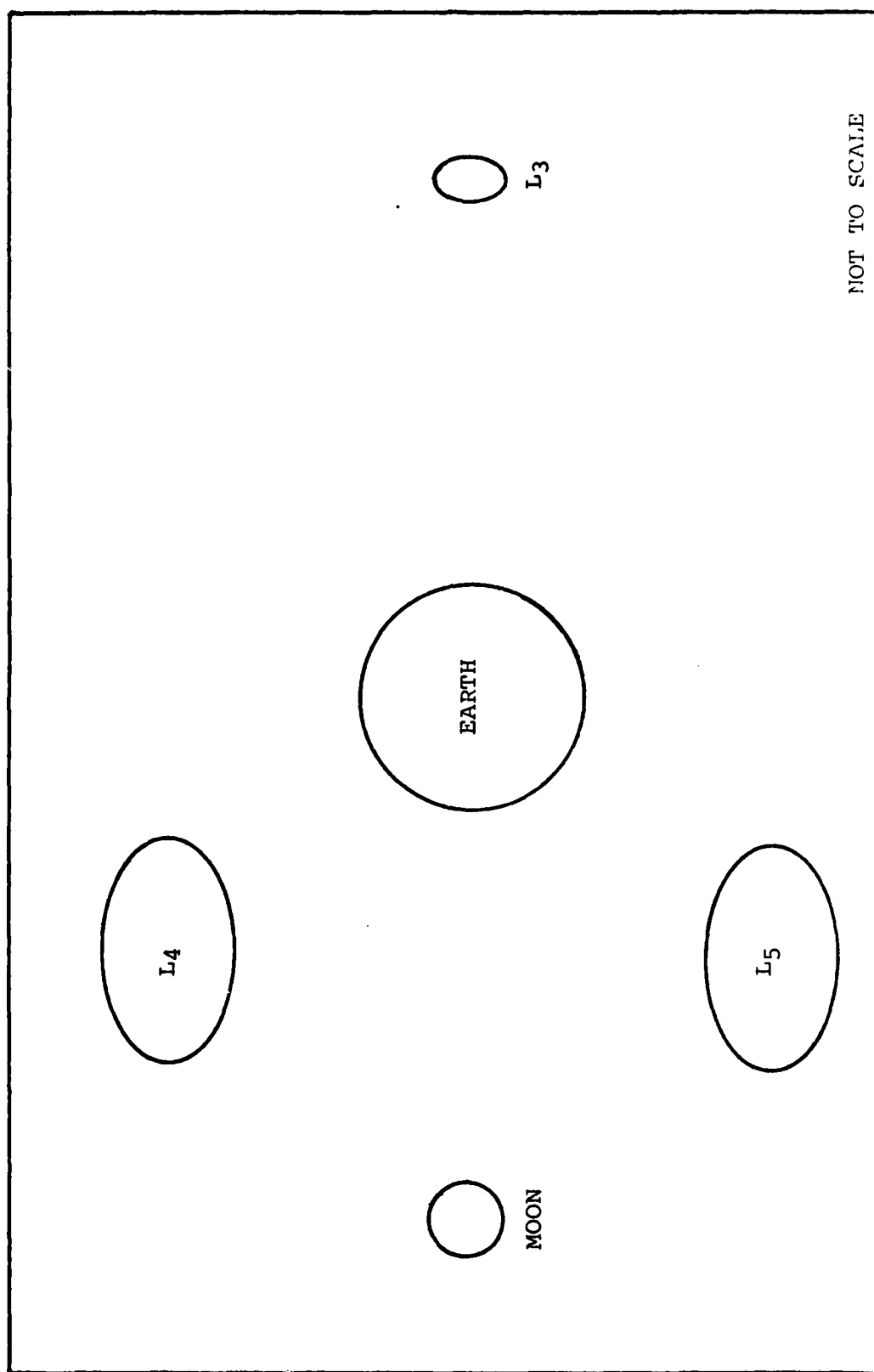
Capt. W. E. Wiesel (Ref 2), in unpublished research, discovered a periodic orbit about L_3 using the same techniques as Capt. Wheeler. It is theorized that if a satellite can be maintained in an orbit about L_3 coupled with satellites in orbit about L_4 and L_5 , then total Earth coverage can be achieved. Figure 1 schematically shows the relative positions of orbits about L_3 , L_4 and L_5 with respect to the Earth. Such coverage could be utilized in world-wide communications. Additionally, intelligence benefits to the military from such strategic orbital positions would be invaluable. T. K. Berge (Ref 3) mentioned this fact in his paper on Lunar Libration Points.

Since transfer trajectory times from Earth to these orbits are approximately two to eight days, significant lead time important for satellite protection and survivability is greatly enhanced. Further, any stabilized orbits in the vicinity of L_3 , L_4 or L_5 would be of great interest to the scientific community for advancing space colonization and deep space studies.

Problem and Scope

Capt. Wiesel (Ref 2) found, as mentioned above, an unstable periodic orbit about L_3 in an idealized model. This

orbit was found by searching for a set of initial conditions that would allow an orbit about L_3 to close on itself. The problem is to derive a linear constant gain feedback control system to stabilize this orbit in a non-idealized model, and to assess the long term control costs associated with such stabilization. The non-idealized model used is not restricted to circular motion but includes the elliptic perturbation caused by the Sun, Moon and Earth. However, all motion is restricted to one plane. Forces due to orbit plane inclination and other planets are neglected as well as other minute forces. A satellite placed in orbit about L_3 in the idealized model will remain in the vicinity of L_3 for approximately four months. However, the same satellite in the same orbit in the non-idealized model would be well on its way out of the Earth-Moon system in one month. Obviously, some sort of control stabilization is needed in practical applications.



II. Problem Analysis

Wheeler Model

Capt. Wheeler (Ref 1) derived the equations of motion for his model using Lagrange's equations. He made several important assumptions concerning the level of complexity. The most important is that satellite motion is governed by the gravitational interaction of the Earth, Moon and Sun in circular orbits. Further, the Earth and Moon rotate about their barycenter with a constant rate; and this barycenter rotates about the Earth/Moon/Sun barycenter with a constant rate. These assumptions allow the calculation of periodic orbits. It should be pointed out that the effects of orbit eccentricity and orbit plane inclinations are not included in the equations of motion, because the effects are small compared to the gravitational forces involved. Also, other small perturbing forces such as the gravitational attraction of other planets, solar wind, radiation pressure, etc. have been omitted. Since orbit plane inclination is small, planar motion was used throughout his report. Capt. Wheeler derived his equations in an inertial reference frame centered at the Earth/Moon/Sun barycenter; but he expressed them in the rotating Earth/Moon coordinate frame centered at the Earth/Moon barycenter. This allows easy visualization of periodic orbits. Lastly, imbedded in all these assumptions is that no control

force is provided by the satellite. This means the satellite will go wherever the forces of the Earth, Moon and Sun direct it to go. Figure 2 is a diagram of the Wheeler restricted four-body coordinate system.

In reality the Wheeler model is very idealized. This idealization is necessary to obtain periodic motion. However, accurate control cost assessment requires a realistic model. Such a model would include the effects of non-circular orbits, non-constant orbit rates and the ability of the satellite to provide control forces.

Heppenheimer Model

In a recent paper on Space Colonization, T. A. Heppenheimer, (Ref 4) presented a more detailed model of the restricted four-body problem. Satellite motion in his model is governed by the gravitational interaction of the Earth, Moon and Sun. In his model the Sun is in an unperturbed elliptic orbit about the Earth/Moon barycenter. Equations of motion for the Moon include the perturbing effects of the Sun's orbit as well as the two-body forces due to the Earth. As in the Wheeler model, the Heppenheimer model also assumes planar motion.

In contrast to the Wheeler model, the Heppenheimer model includes all of the major disturbing forces due to orbit eccentricity. Those forces not accounted for in the Heppenheimer model are: forces due to orbit plane inclination, other planets, solar wind and radiation pressure. A complete derivation

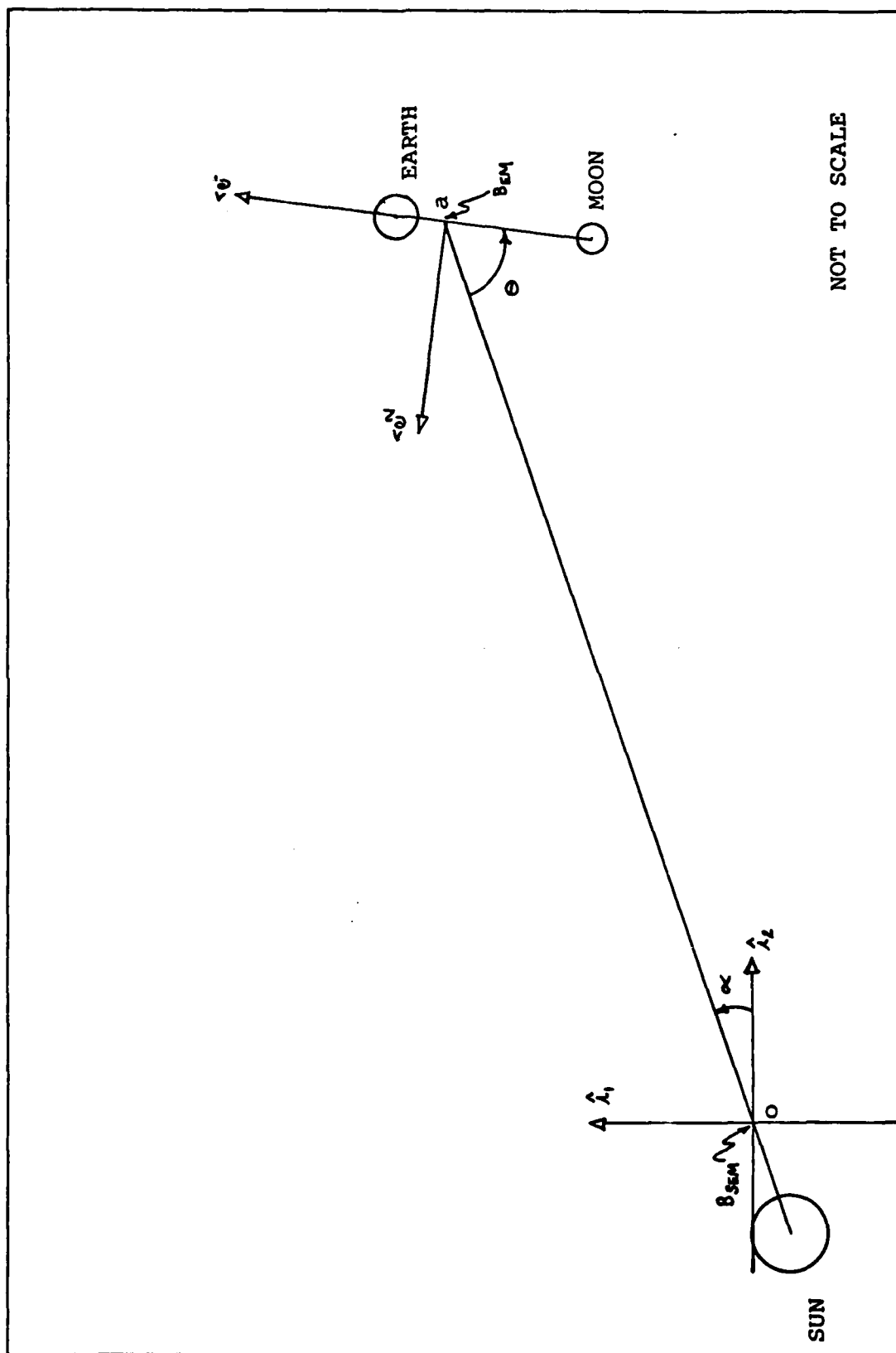


Fig 2. Wheeler Four-Body Coordinate System

of the Heppenheimer equations of motion is included in Appendix A. A diagram of the Heppenheimer four-body coordinate system is shown in Figure 3.

A weakness of the Heppenheimer model is that the equations of motion are expressed in a non-rotating Earth centered coordinate frame. With this coordinate frame visualization of periodic orbits is difficult at best. Therefore, illustration of the relative sizes and shapes of orbits computed in the Heppenheimer model will be projected in the Wheeler rotating coordinate frame.

Coordinate Transformation

Figure 4 illustrates the relative orientation of the Heppenheimer coordinate frame superimposed on the Wheeler coordinate frame. The following subscripts refer to points used: a - origin of Wheeler Earth/Moon system; b - origin of Heppenheimer system; o - origin of the inertial system; and p - satellite position. For example $\underline{r}_{p/a}$ should be read as: the position of point p with respect to point a. Additionally, $\hat{\alpha}_i$ and $\hat{\epsilon}_i$ represent unit vectors in the Heppenheimer and Wheeler systems, respectively. Equation (1) describes the relative position vector between Wheeler and Heppenheimer coordinates

$$\underline{r}_{p/a} = \underline{r}_{p/b} + \underline{r}_{b/a} \quad (1)$$

where

$$\underline{r}_{p/a} = x_{\epsilon} \hat{\epsilon}_1 + y_{\epsilon} \hat{\epsilon}_2 \quad (2)$$

$$\underline{r}_{p/b} = x_{\alpha} \hat{\alpha}_1 + y_{\alpha} \hat{\alpha}_2 \quad (3)$$

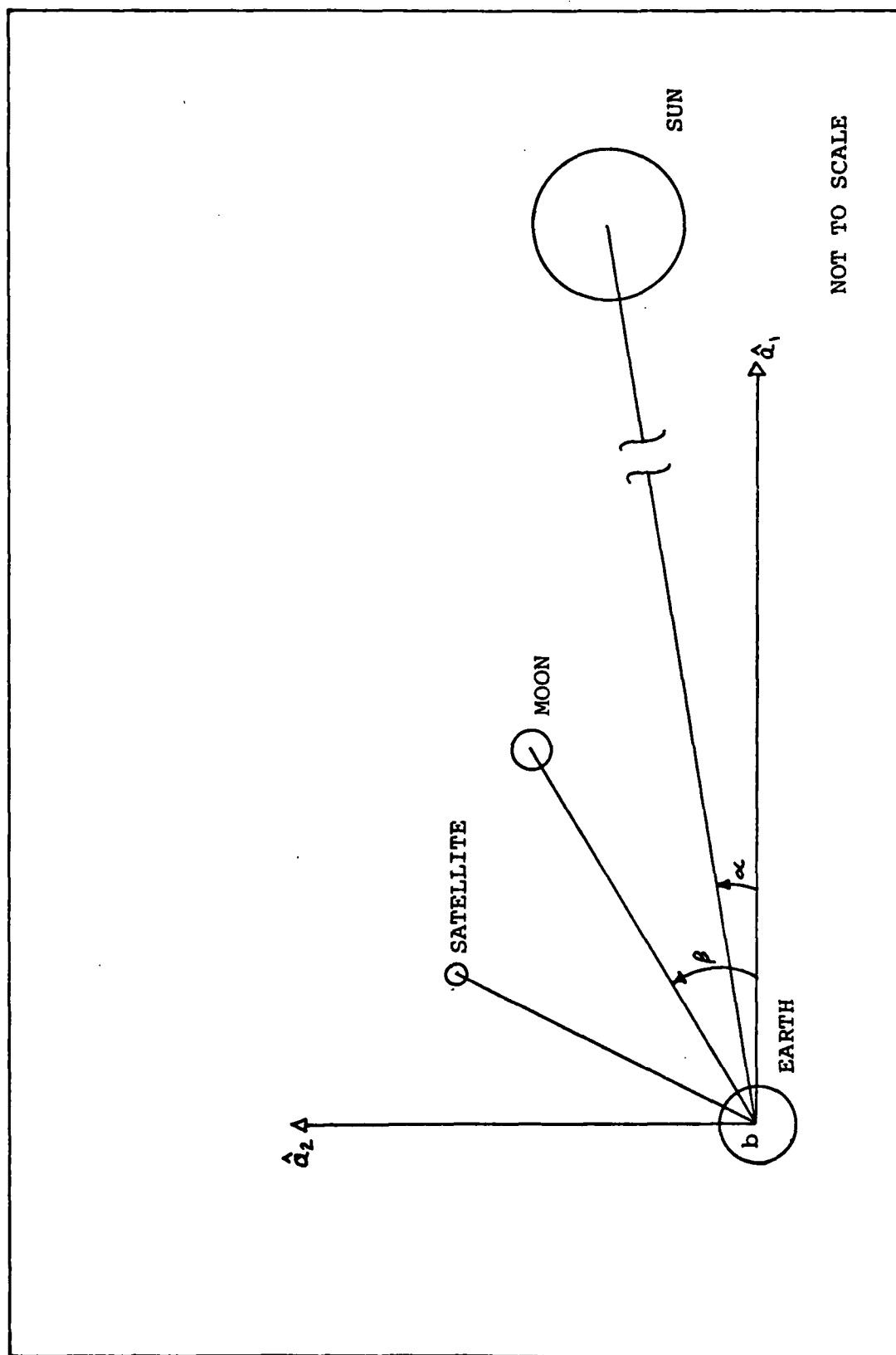


Fig 3. Heppenheimer Four-Body Coordinate System

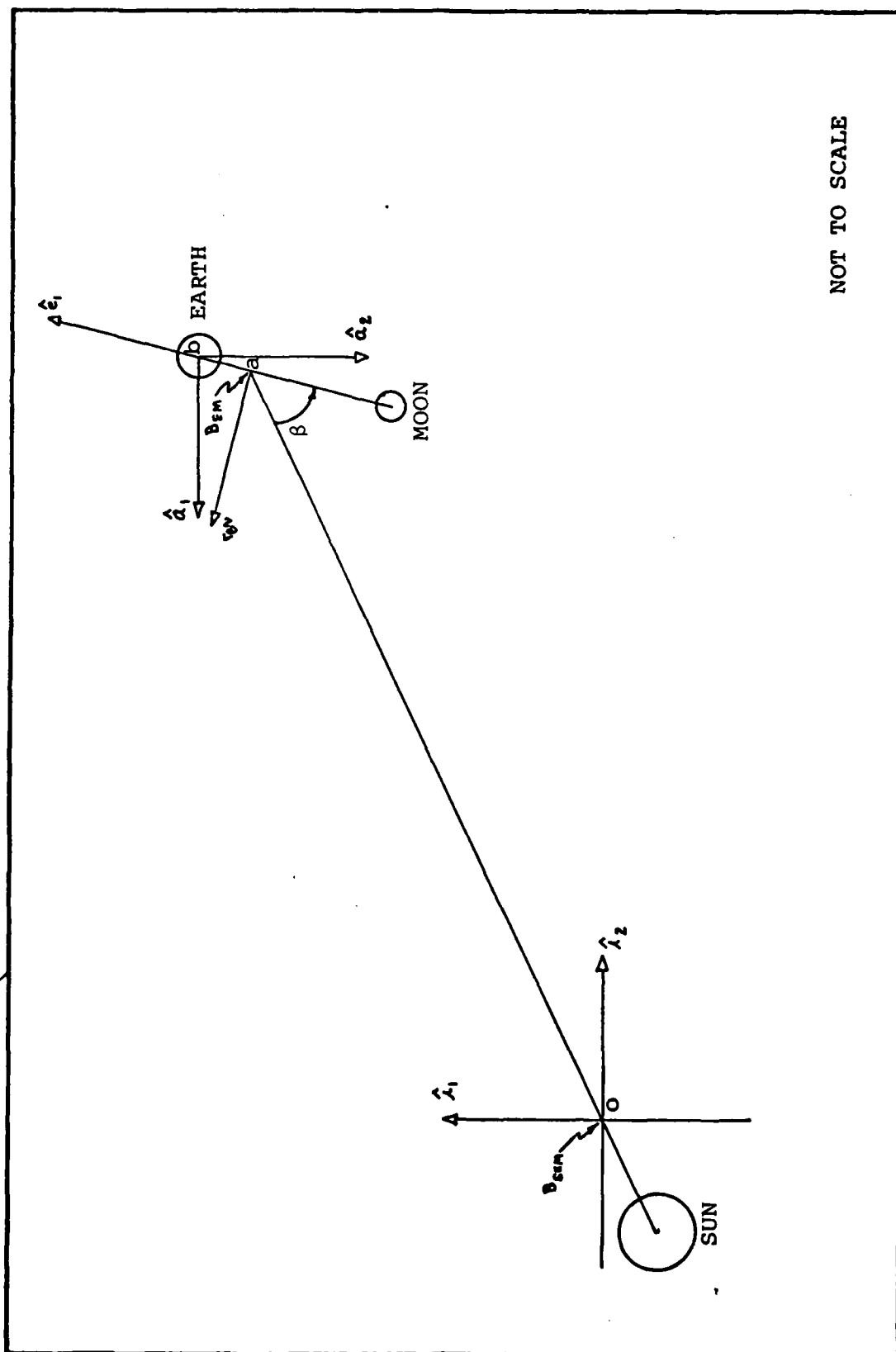


Fig 4. Combined Heppenheimer/Wheeler
Coordinate Systems

$$\underline{r}_{b/a} = \mu \hat{e}_1 \quad (4)$$

Solving Equation (1) for $\underline{r}_{p/b}$ and substituting in (2), (3) and (4) yields

$$X_\alpha \hat{a}_1 + Y_\alpha \hat{a}_2 = (X_\epsilon - \mu) \hat{e}_1 + Y_\epsilon \hat{e}_2 \quad (5)$$

The Heppenheimer X_α coordinate in terms of Wheeler coordinates can be found by vector dot of both sides of Equation (5) with \hat{a}_1 . Likewise, the Y_α coordinate can be found by taking the dot product of both sides of (5) with \hat{a}_2 . The results are

$$X_\alpha = (\mu - X_\epsilon) \cos \beta + Y_\epsilon \sin \beta \quad (6)$$

$$Y_\alpha = (\mu - X_\epsilon) \sin \beta - Y_\epsilon \cos \beta \quad (7)$$

Recalling Figure 4, the initial position transformations can be found when $t = 0$, which implies $\beta = 0$. Then

$$X_\alpha = \mu - X_\epsilon \quad (8)$$

$$Y_\alpha = -Y_\epsilon \quad (9)$$

The initial velocity conditions can be transformed in a similar fashion. The following superscripts refer to the reference coordinate frame used: a - Heppenheimer, e - Wheeler, and i - inertial. For example $\underline{v}_{p/o}^i$ should be read as: the velocity of point p with respect to point o as seen by an observer in frame i.

The inertial velocity of a satellite in the Wheeler frame is given by

$$\underline{v}_{p/o}^i = \underline{v}_{p/a}^i + \underline{v}_{a/o}^i \quad (10)$$

where

$$\underline{v}_{p/a}^i = \underline{v}_{p/a}^e + \underline{\omega}^{ei} \times \underline{r}_{p/a} \quad (11)$$

Substitution of (11) into (10) yields

$$\underline{v}_{p/o}^i = \underline{v}_{p/a}^e + \underline{\omega}^{ei} \times \underline{r}_{p/a} + \underline{v}_{a/o}^i \quad (12)$$

Similarly, the inertial velocity of a point in the Heppenheimer frame is

$$\underline{v}_{p/o}^i = \underline{v}_{p/b}^i + \underline{v}_{b/o}^i \quad (13)$$

where

$$\underline{v}_{p/b}^i = \underline{v}_{p/b}^a + \underline{\omega}^{ai} \times \underline{r}_{p/b} \quad (14)$$

$$\underline{v}_{b/o}^i = \underline{v}_{b/a}^i + \underline{v}_{a/o}^i \quad (15)$$

and

$$\underline{v}_{b/a}^i = \underline{v}_{b/a}^e + \underline{\omega}^{ei} \times \underline{r}_{b/a} \quad (16)$$

Substitution of (14), (15) and (16) into (13) yields

$$\underline{v}_{p/o}^i = \underline{v}_{p/b}^a + \underline{\omega}^{ai} \times \underline{r}_{p/b} + \underline{v}_{b/a}^e + \underline{\omega}^{ei} \times \underline{r}_{b/a} + \underline{v}_{a/o}^i \quad (17)$$

Equating (12) and (17) and solving for $\underline{v}_{p/b}^a$ gives

$$\underline{v}_{p/b}^a = \underline{v}_{p/a}^e - \underline{v}_{b/a}^e - \underline{\omega}^{ai} \times \underline{r}_{p/b} - \underline{\omega}^{ei} \times \underline{r}_{p/a} - \underline{\omega}^{ei} \times \underline{r}_{b/a} \quad (18)$$

Since $\underline{\omega}^{ai} = 0$ in the Heppenheimer frame and $\underline{v}_{b/a}^e = 0$ in the Wheeler frame equation (18) reduces to

$$\underline{v}_{p/b}^a = \underline{v}_{p/a}^e + \underline{\omega}^{ei} \times \underline{r}_{p/a} - \underline{\omega}^{ei} \times \underline{r}_{b/a} \quad (19)$$

Equation (19) gives the Heppenheimer velocity in terms of the Wheeler velocity, position and angular coordinates. One additional transformation is needed. Since the Wheeler time unit is based on the synodic period and the Heppenheimer time unit is based on the sidereal period, the Wheeler velocity must be

multiplied by the value of the sidereal period divided by the synodic period. That is

$$dt_w = 27.32166101 \text{ days per synodic month (Ref 5:334)}$$

and

$$dt_h = 29.5303882 \text{ days per sidereal month (Ref 5:334)}$$

where the subscript w refers to Wheeler time and h to Heppenheimer time. Then

$$\frac{dr}{dt_h} = \frac{dr}{dt_w} \left(\frac{dt_w}{dt_h} \right) = \frac{dr}{dt_w} (.9251986728) \quad (20)$$

letting

$$\frac{dt_w}{dt_h} = S_f = .9251986728 \quad (21)$$

Integrating (20) and (21) into (19) gives

$$\underline{v}_{p/b}^a = \underline{v}_{p/a}^e (S_f) + \underline{\omega}^{ei} \times \underline{r}_{p/a} - \underline{\omega}^{ei} \times \underline{r}_{b/a} \quad (22)$$

Writing equation (22) in vector components, performing the indicated operations and finally dotting both sides with \hat{a}_1 , then \hat{a}_2 yields, respectively

$$\dot{x}_\alpha = \{Y_\epsilon \dot{\theta} - \dot{X}_\epsilon (S_f)\} \cos \beta + \{\dot{Y}_\epsilon (S_f) - (\mu - X_\epsilon) \dot{\theta}\} \sin \beta \quad (23)$$

$$\dot{y}_\alpha = \{Y_\epsilon \dot{\theta} - \dot{X}_\epsilon (S_f)\} \sin \beta - \{\dot{Y}_\epsilon (S_f) - (\mu - X_\epsilon) \dot{\theta}\} \cos \beta \quad (24)$$

Recalling Figure 4, the initial velocity transformations can be found when $t = 0$ which implies $\beta = 0$. With $\dot{\theta} = 1$, a value which is the constant rate in the Wheeler model, Equations (23) and (24) reduce to

$$\dot{x}_\alpha = Y_\epsilon - \dot{X}_\epsilon (S_f) \quad (25)$$

$$\dot{y}_\alpha = \mu - X_\epsilon - \dot{Y}_\epsilon (S_f) \quad (26)$$

Equations (8), (9), (25) and (26) will be used at a later time to transform Wheeler initial conditions into Heppenheimer initial conditions.

Verification of the Reduced

Heppenheimer Equations of Motion

Before proceeding into a detailed analysis of the problem, there are certain routines and equations that need to be verified. Comparison of a known solution with the solution generated by the Heppenheimer model will verify that Heppenheimer equations have been correctly programmed. A logical choice for this comparison is the Wheeler L_4 solution. Reduction of the Heppenheimer model to an equivalent Wheeler model requires setting the eccentricity of the Sun to zero, a value that causes circular motion. Also the mass of the Sun is set to zero in the equations of motion for the Moon. This effectively removes the Sun's perturbation upon the Moon's orbit and enables the Moon to have a circular orbit provided that the proper initial condition for the Moon's velocity is chosen. The velocity required for a circular orbit of radius r can be calculated from the energy equation for two-body motion which is

$$E = \frac{V^2}{2} - \frac{\mu}{r} = - \frac{\mu}{2a} \quad (\text{Ref 9:34})$$

For circular orbits $r = a$, then circular velocity becomes

$$V_c = \sqrt{\mu/r}$$

For this specific case $\mu = 1$, the mass of the Moon plus the mass of the Earth. Also, $r = 1$, the distance from the Earth

to the Moon. Therefore, the required circular velocity of the Moon is

$$V_C = \sqrt{1/1} = 1$$

Recalling Equation (A-11) and applying the above simplifications, the reduced Heppenheimer equations of motion are

$$\ddot{X}_m + \frac{X_m}{R_m^3} = 0 \quad (27)$$

$$\ddot{Y}_m + \frac{Y_m}{R_m^3} = 0 \quad (28)$$

$$\ddot{X}_C = - \frac{(1-\mu)}{r_C^3} X_C - M_S \left(\frac{X_C - X_S}{r_{CS}^3} + \frac{X_S}{r_S^3} \right) - \mu \left(\frac{X_C - X_m}{r_{cm}^3} + \frac{X_m}{r_m^3} \right) \quad (29)$$

$$\ddot{Y}_C = - \frac{(1-\mu)}{r_C^3} Y_C - M_S \left(\frac{Y_C - Y_S}{r_{CS}^3} + \frac{Y_S}{r_S^3} \right) - \mu \left(\frac{Y_C - Y_m}{r_{cm}^3} + \frac{Y_m}{r_m^3} \right) \quad (30)$$

where the subscripts c, s, and m stand for satellite, Sun, and Moon, respectively.

Capt. Wheeler (Ref 1:62) gives the initial conditions for periodic satellite motion about L_4 as

$$X_E = -.72418782459$$

$$Y_E = .81568639689$$

$$\dot{X}_E = .07948061949$$

$$\dot{Y}_E = .22438007788$$

Recalling equations (8), (9), (25) and (26) where $\mu = .0121396054$ (Ref 6:517), the equivalent Heppenheimer L_4 initial conditions are

$$X_\alpha = .73632742991 \quad (31)$$

$$Y_\alpha = -.81568639689 \quad (32)$$

$$\dot{X}_\alpha = .74215103322 \quad (33)$$

$$\dot{Y}_\alpha = .52873127973 \quad (34)$$

Analogously, Capt. Wiesel (Ref 2) gives the initial conditions for L_3 as

$$X_{\epsilon} = .9967446273$$

$$Y_{\epsilon} = 0.$$

$$\dot{X}_{\epsilon} = 0.$$

$$\dot{Y}_{\epsilon} = .0210258862$$

Thus, the equivalent Heppenheimer L_3 initial conditions are

$$X_{\alpha} = -.9846050219 \quad (35)$$

$$Y_{\alpha} = 0. \quad (36)$$

$$\dot{X}_{\alpha} = 0. \quad (37)$$

$$\dot{Y}_{\alpha} = -1.004058144 \quad (38)$$

Numerically integrating equations (27) through (30) with initial conditions (31) through (34) for one period did result in the same periodic orbit about L_4 as found by Capt. Wheeler (Ref 1:63). As a further check the same procedure is applied to L_3 using initial conditions (35) through (38). After the end of one period, the Heppenheimer model did reproduce the same orbit discovered by Capt. Wiesel. It should be noted that one period in the Wheeler model is 2π radians; but due to the different time scales, one period in the Heppenheimer system is

$$\tau_h = \tau_w \left(\frac{dt_w}{dt_h} \right) = \frac{\tau_w}{S_f} \quad (39)$$

$$\tau_h = \frac{2\pi}{S_f} = 6.791174148 \quad (40)$$

Figure 5 represents the L_4 orbit presented by Capt. Wheeler (Ref 1:63), and Figure 6 is the same L_4 orbit generated by the reduced Heppenheimer model. Figure 7 is the L_3 orbit

discovered by Capt. Wiesel, and Figure 8 is the same L_3 orbit generated by the reduced Heppenheimer model. Even though the reduced Heppenheimer model is able to accurately reproduce known solutions as shown above, no known solution exists for the complete Heppenheimer model.

One final check on the correct implementation of the complete Heppenheimer model is needed. It is reasoned that over a long period of time the motion produced by each model should be drastically different. This difference is caused by the fact that the Heppenheimer model is a "real world" model; while the Wheeler model is only an idealized version of the Heppenheimer model. For comparison each model was run for four months. Figure 9 shows the unstable but "semi" orderly motion of the L_3 orbit in the Wheeler model as it departs the Earth-Moon system. Figure 10, on the other hand, illustrates the catastrophic instability of the same L_3 orbit when run in the realistic Heppenheimer model.

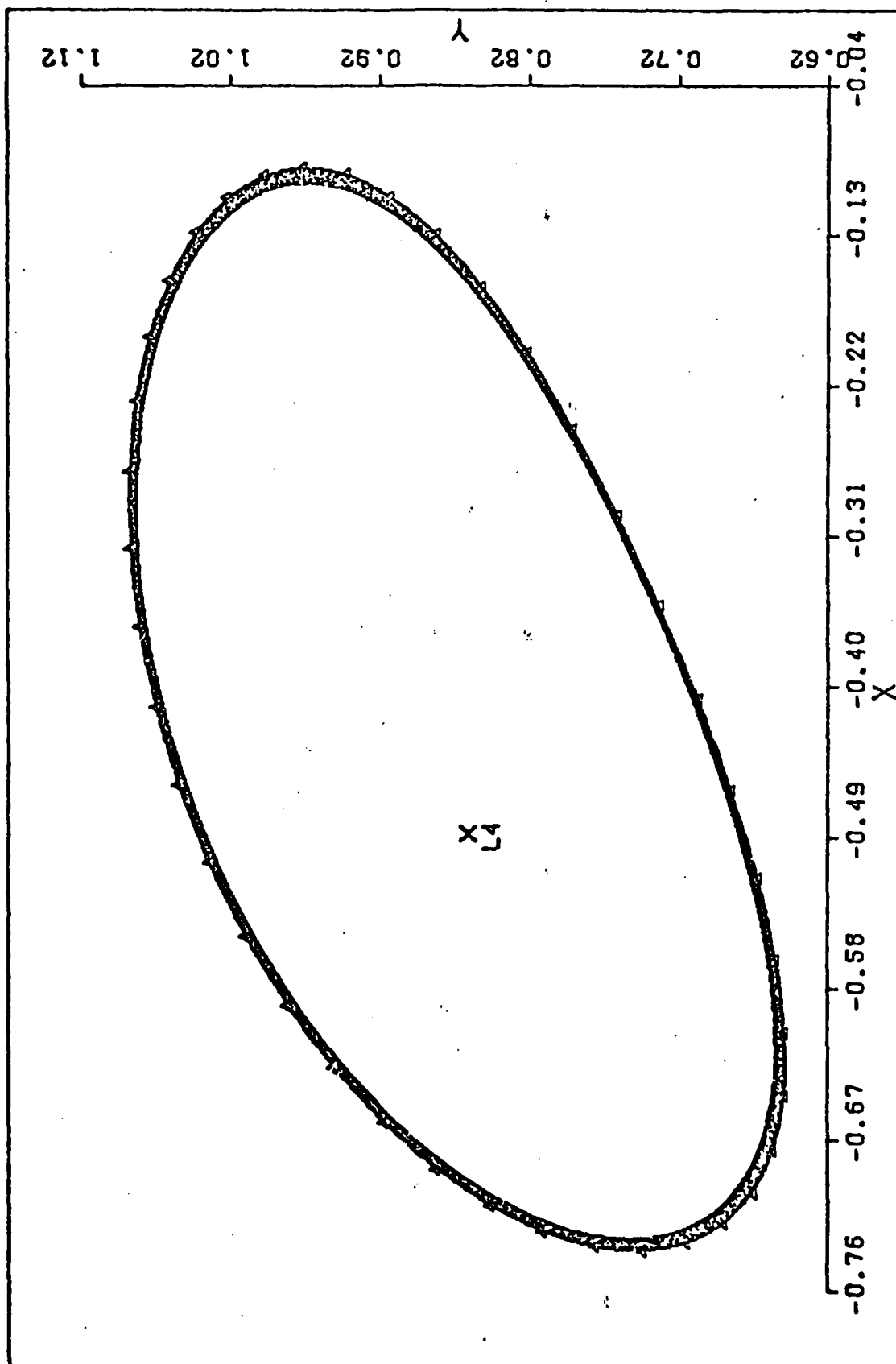


Fig 5. L_4 Orbit using the Wheeler Model

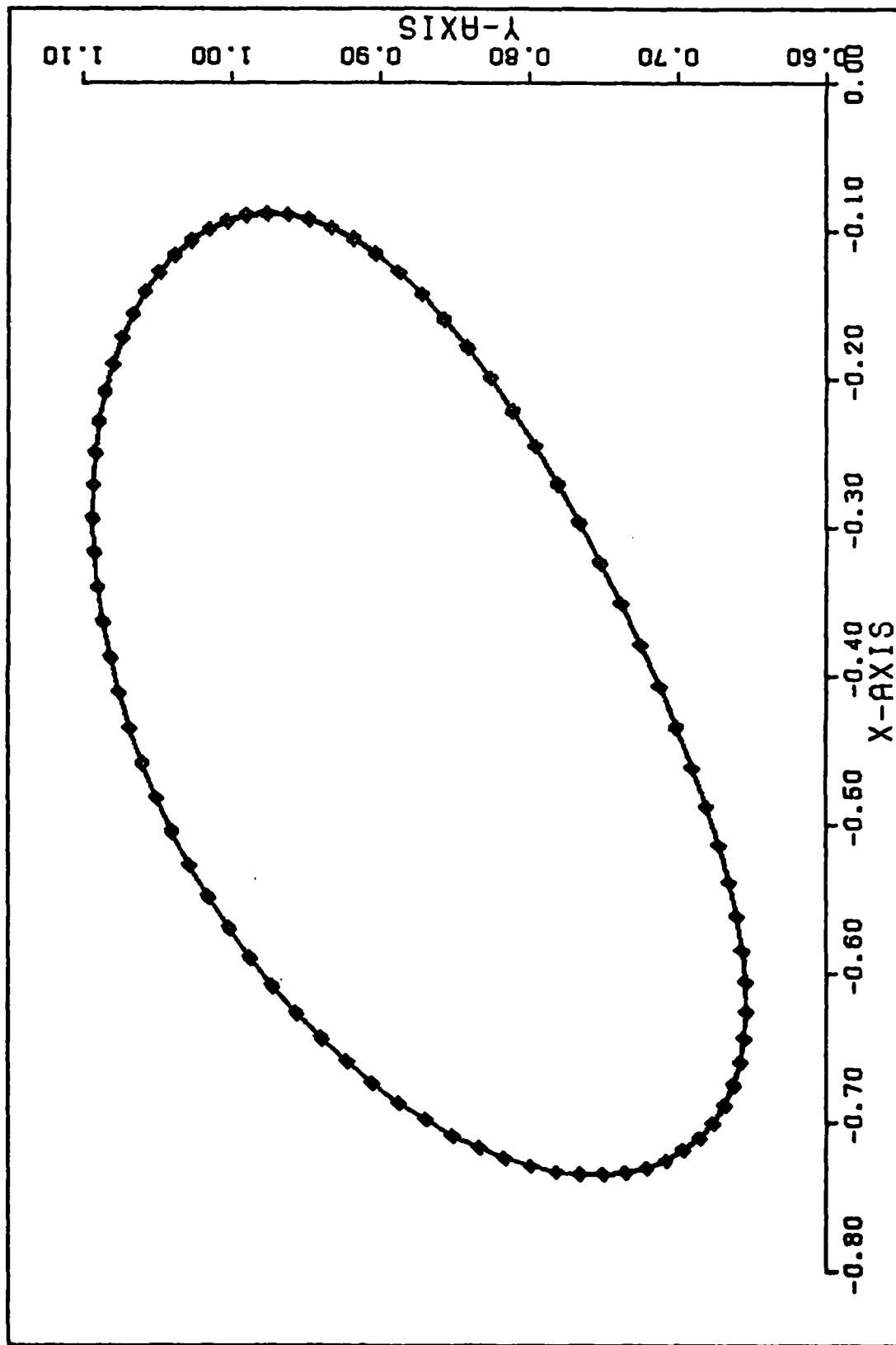


Fig 6. L_4 Orbit using the Reduced
Heppenheimer Model

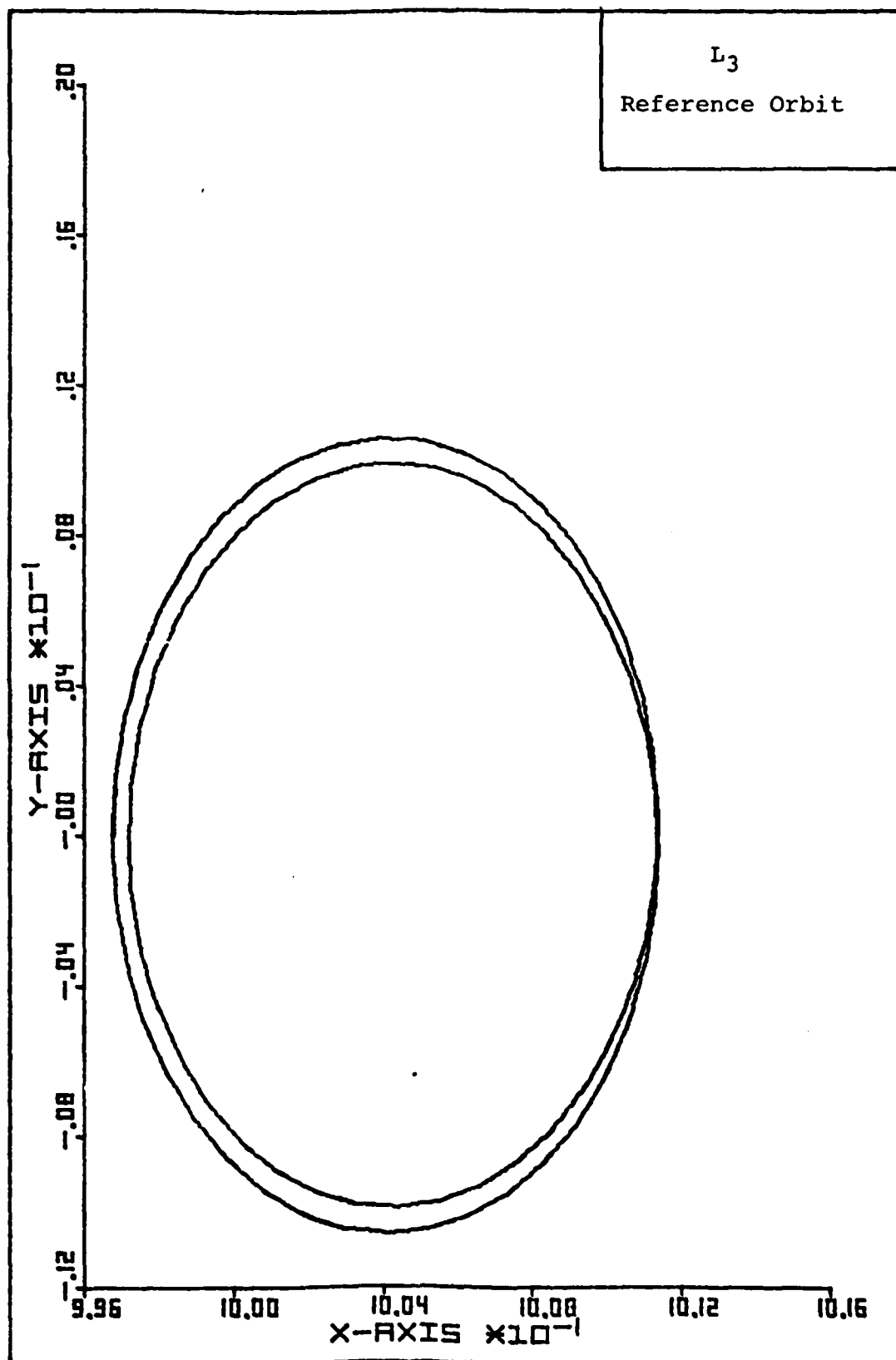


Fig. 7 L_3 Orbit Discovered by Capt Wiesel

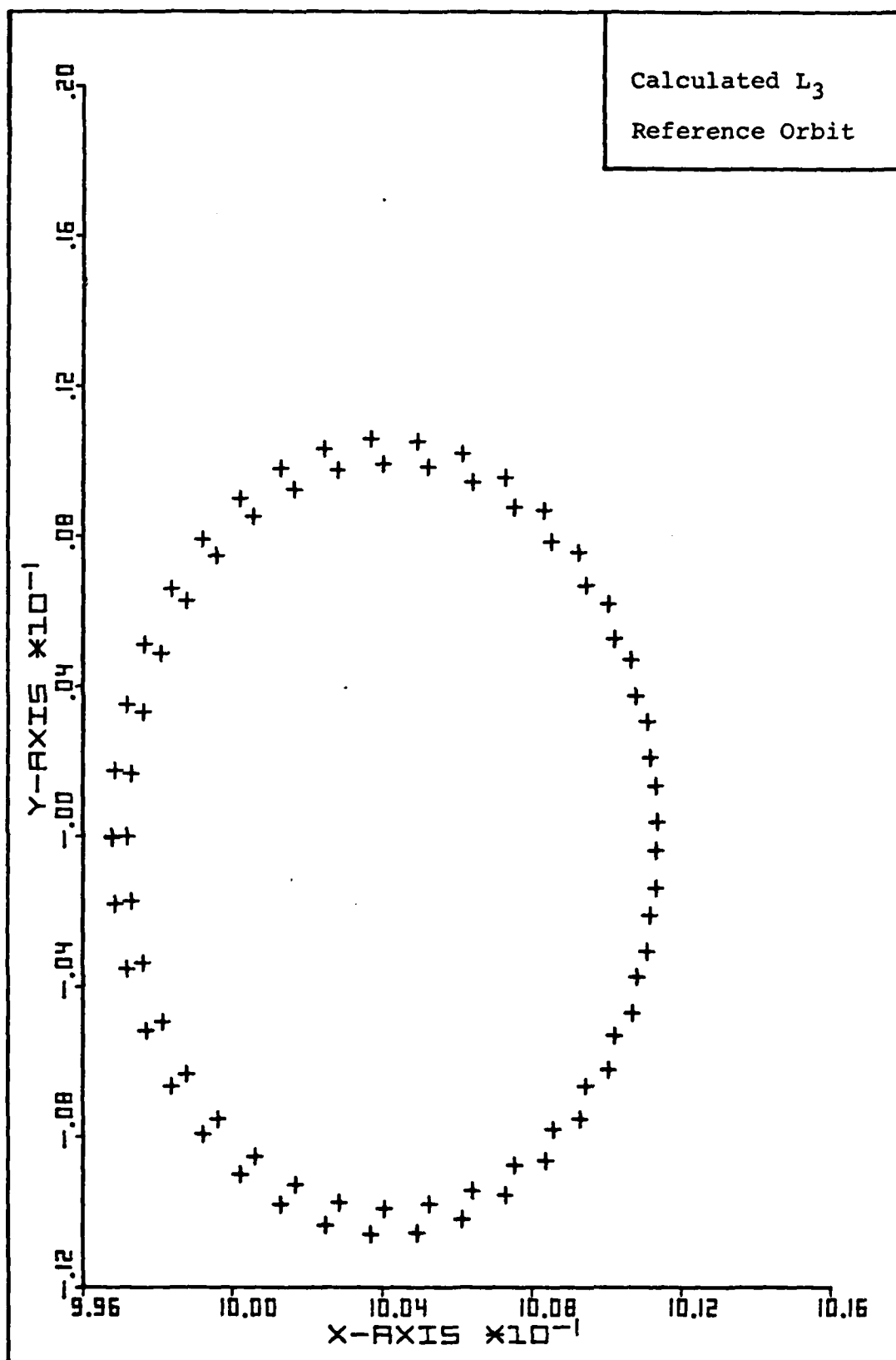


Fig. 8 L_3 Orbit using the Reduced Heppenheimer Model

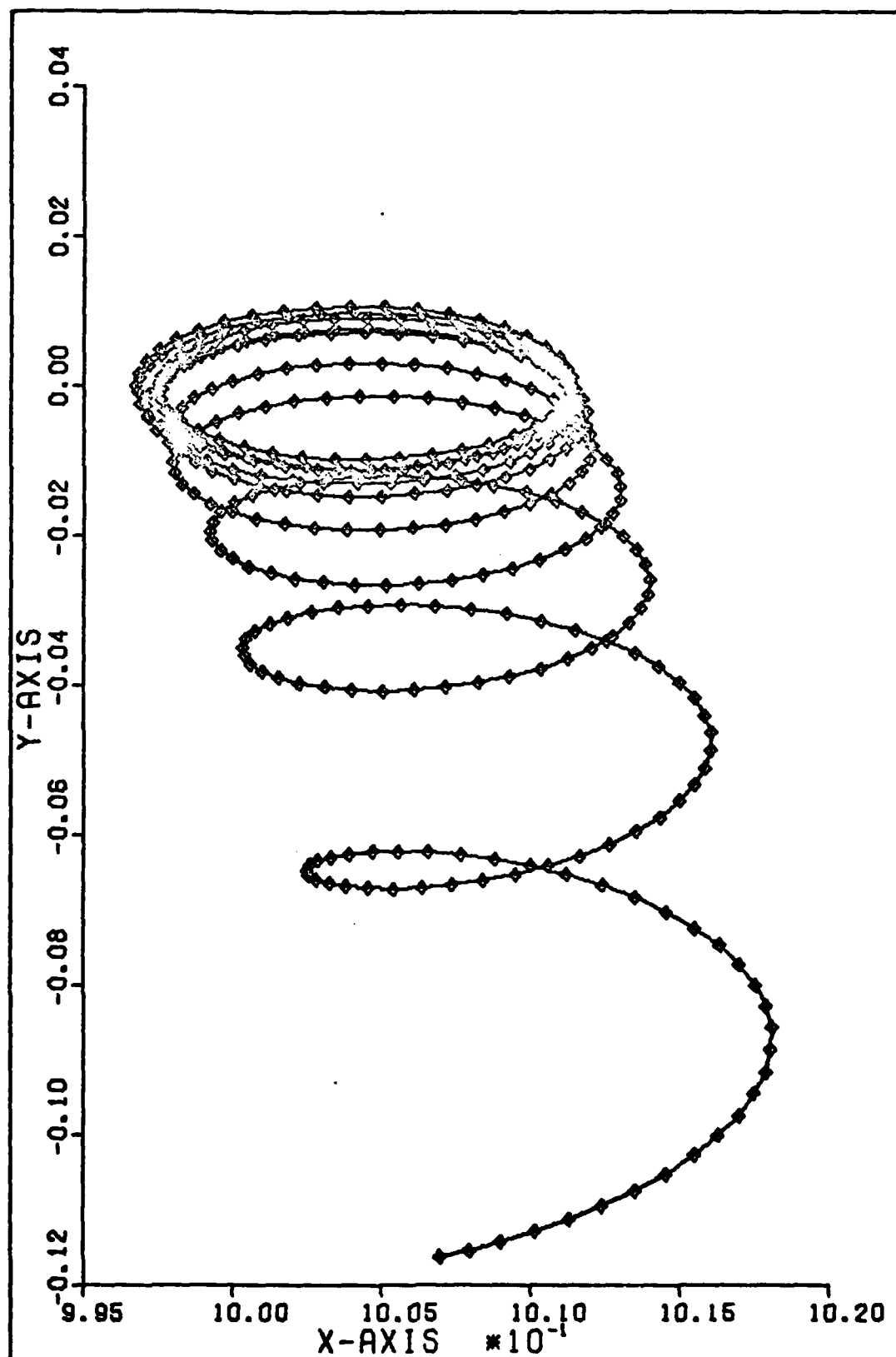


Fig 9. L₃ Orbit using the Wheeler Model
for four months

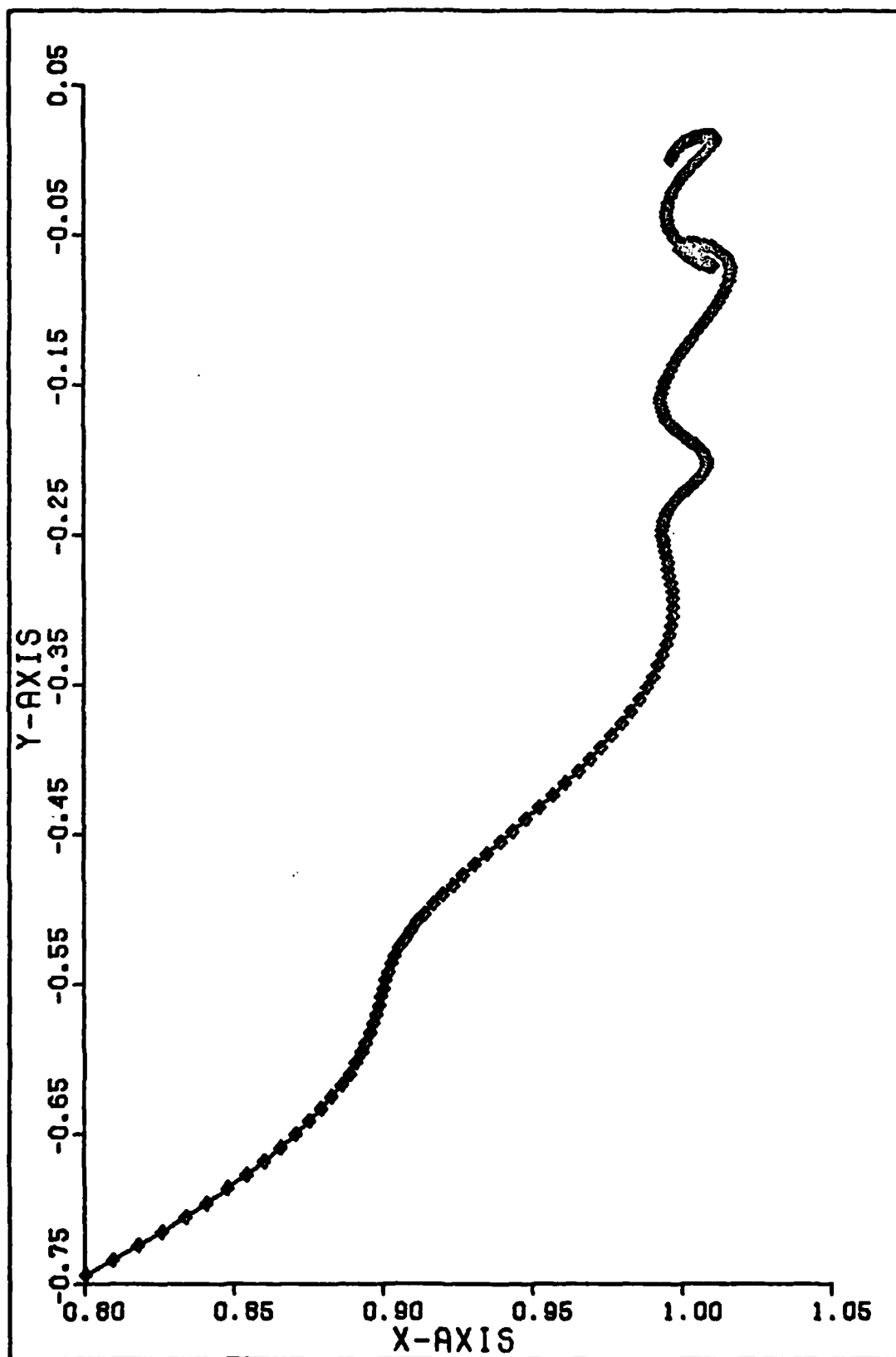


Fig 10. L_3 Orbit using the Heppenheimer Model
for four months

III. Feedback Control

Stability of Periodic Orbits

In general the second-order non-linear differential equations of motion can be cast into a set of first order non-linear differential equations with the form

$$\dot{\underline{X}}(t) = f(\underline{X}(t), t) \quad (41)$$

which states that the first order non-linear equations of motion are functions of the states themselves and time.

For small displacements from the states at any time, t , equation (41) becomes

$$\dot{\underline{X}}(t) + \delta\dot{\underline{X}}(t) = f(\underline{X}(t) + \delta\underline{X}(t), t) \quad (42)$$

Expanding the right side of (42) as a Taylor series in $\delta\underline{X}(t)$ results in

$$\begin{aligned} \dot{\underline{X}}(t) + \delta\dot{\underline{X}}(t) &\approx f(\underline{X}(t), t) + \frac{\partial f}{\partial \underline{X}(t)} \delta\underline{X}(t) \\ &\quad + \text{higher order terms} \end{aligned} \quad (43)$$

Neglecting higher order terms and recalling (41), equation (43) reduces to

$$\delta\dot{\underline{X}}(t) = \frac{\partial f}{\partial \underline{X}(t)} \delta\underline{X}(t) \quad (44)$$

Which relates small displacements in the states to changes in the equations of motion. As a simplifying step, let

$$A(t) = \frac{\partial f}{\partial \underline{X}(t)}$$

Where the components of

$$A(t), [A_{ij}] = \frac{\partial f_i}{\partial x_j}$$

are partial derivatives of the equations of motion with respect to the individual states. In this case $A(t)$ is not only time varying, but also periodic.

Meirovitch (Ref 7:264) states that a general solution to Equation (44) when evaluated along a periodic orbit is

$$\delta \underline{X}(t) = \sum_{j=1}^N \underline{Q}_j(t) e^{\sigma_j t} \quad (45)$$

The quantities σ_j are called the Poincaré or characteristic exponents. Matrix \underline{Q}_j represents the direction and magnitudes of oscillation about the equilibrium point. As stated, equation (45) relates the deviation from a periodic orbit as a function of the Poincaré exponents. It can also be shown that

$$\delta \underline{X}(t) = \Phi(t,0) \delta \underline{X}(0) \quad (46)$$

Where Φ is the monodromy matrix, or more commonly referred to as the state transition matrix. Combining equations (45) and (46) and evaluating after one period, τ , yields

$$\delta \underline{X}(\tau) = \underline{Q}_j(\tau) e^{\sigma_j \tau} = \Phi(\tau,0) \underline{Q}_j(0) \quad (47)$$

Utilizing the fact that $\underline{Q}_j(\tau)$ is periodic and rearranging gives

$$\{\Phi(\tau,0) - e^{\sigma_j \tau} I\} \underline{Q}_j(0) = 0 \quad (48)$$

Obviously equation (48) represents an eigenvalue problem where the eigenvalues of $\Phi(\tau,0)$ are

$$\lambda_i = e^{\sigma_j \tau} \quad (49)$$

Solving equation (49) for the Poincaré exponent gives

$$\sigma_j = \frac{1}{\tau} \log \lambda_i \quad (50)$$

Since for this problem equation (44) represents a Hamiltonian system, Meirovitch (Ref 7:275) further states that the characteristic exponents for such a system occur in positive and negative pairs. For stability, in a linear sense, the real part of the σ_j 's determines the stability. Thus, any negative real part implying stability automatically carries with it a conjugate of the opposite sign implying instability.

Since the orbit about L_3 is unstable, it is obvious that at least one pair of σ_j 's have non-zero real parts. Orbital stability in a linear sense is achieved by reducing these non-zero values to purely imaginary. The simplest means would be with linear constant gain feedback control. However, using feedback control causes the dynamical system to become non-Hamiltonian. Therefore, the minimum criteria for stability is now that all σ_j 's must be purely imaginary. When all σ_j 's are purely imaginary, the system exhibits "critical behavior." In this case the system can be either stable or unstable depending upon the higher order terms, which were neglected in the linearization. When all σ_j 's possess negative real parts, then the system is "asymptotically stable."

Feedback Compensation

Compensation of a system by adding poles and zeros is used to improve system performance. Three types of state feedback compensation systems will be analyzed for cost and effectiveness.

They are position, velocity and position/velocity. Since a measure of cost is the total control gain per unit time needed to maintain orbital stability; the stabilizing effects of feedback compensation are first verified using the Wheeler model. If stability in the Wheeler model cannot be achieved, it is futile to attempt to stabilize the Heppenheimer model. Logically, stability in the Wheeler model does not necessarily imply stability in the Heppenheimer model; or even if stability can be achieved in the Heppenheimer model it may prove to be too costly.

The entire impetus with feedback control is to drive the deviation from the reference orbit to zero or at least to some minimum. In some instances two different values of gain will cause the same amount of deviation. In these instances control gain costs will be the deciding factor. This intuitive optimization scheme is shown in Figure 11. Combinations of deviation and control gain costs in sub-area A are considered to be more effective than those in sub-area B. Hence, the overall underlying theme of this report is that stabilization is more important than control gain cost. Thus, if a choice between two identical orbits with different values of feedback gains is available; the one with the lower control gain cost will be chosen. Since no formal optimization is attempted in this report, the measure of deviation from the reference is left to personal judgement. Since this is an orbiting satellite, control must be applied as an acceleration. Over the long term control gain costs are calculated by

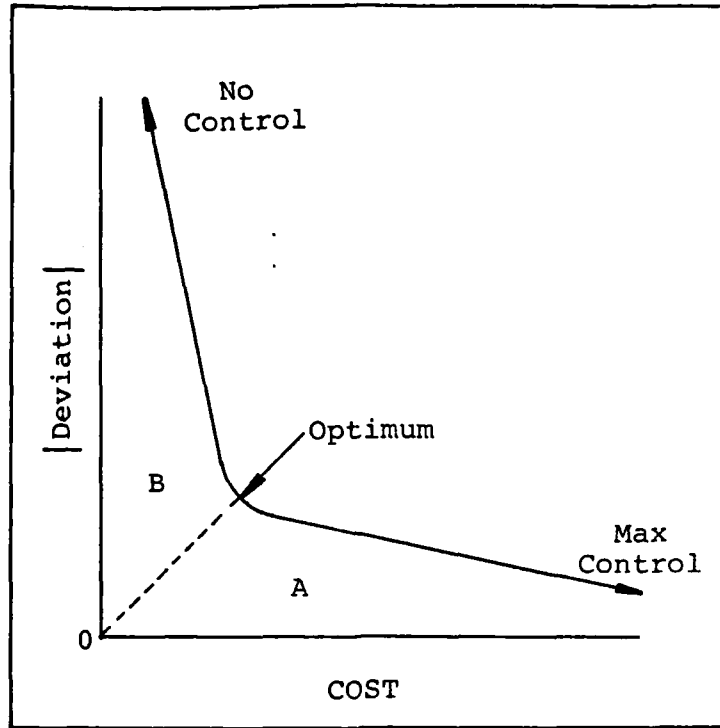


Fig 11. "Quasi" Optimization Scheme

$$C_c = \frac{1}{T} \int_0^T |a_T| dt \quad (51)$$

where

$$a_T = K_p \sqrt{\Delta X^2 + \Delta Y^2} + K_r \sqrt{\Delta \dot{X}^2 + \Delta \dot{Y}^2}$$

this is shown schematically in the lower portion of Figure 12. Crudely, this control cost can be interpreted as an average acceleration requirement. The simplest feedback control system to design is a constant gain system, which is shown schematically in the upper portion of Figure 12.

Recalling equation (44)

$$\delta \dot{\underline{X}}(t) = [\underline{A}(t)] \delta \underline{X}(t)$$

and adding a constant gain feedback matrix K yields

$$\delta \dot{\underline{X}}(t) = [\underline{A}(t)] \delta \underline{X}(t) + [\underline{K}] \delta \underline{X}(t) \quad (52)$$

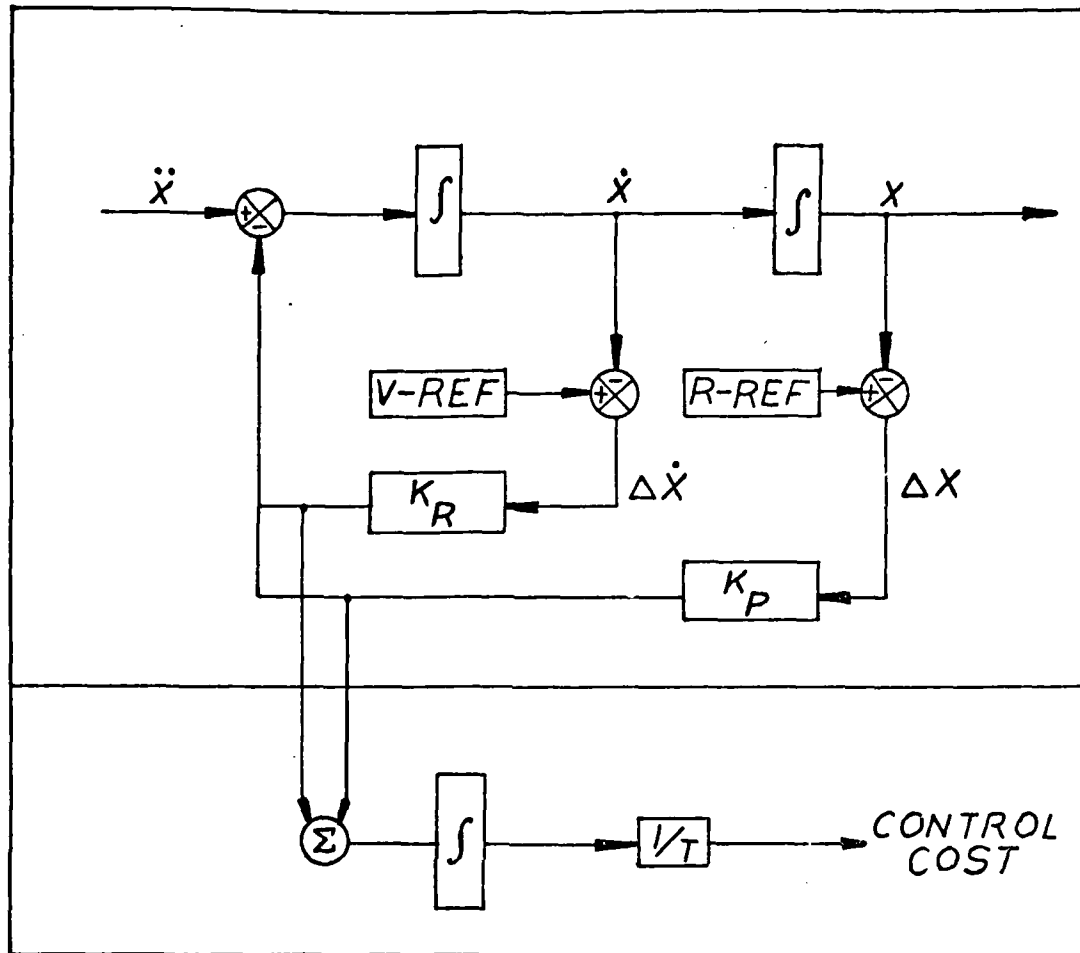


Fig. 12 Feedback Control Diagram

Simplifying (52) gives

$$\delta \dot{\underline{x}}(t) = \{ [\underline{A}(t)] + [\underline{K}] \} \delta \underline{x}(t) \quad (53)$$

The stability of (53) cannot be determined with standard root locus techniques because the $[\underline{A}(t)]$ matrix is not constant but time-varying and periodic. However, recalling that Poincaré exponents are indicators of stability, a "quasi" root locus can be made by solving (53) for the Poincaré exponents and plotting them as a function of feedback gain. Future references to root locus should be understood to mean "quasi" root locus. The elements of $[\underline{K}]$ determine which states will be

used in the feedback loop. Specifically, the effect of position state feedback on orbital stability can be observed with one set of $[K]$ elements. Likewise, effects of velocity state feedback can be seen with a different set of elements; or combining the two, the effects of position and velocity feedback can be observed. The resultant root locus plots of the Wheeler model using position, velocity and position/velocity feedback are shown in Figures 13 to 15, respectively. Note that Figures 13 and 14 are schematic representations of the root locus using position and velocity feedback, respectively. Figure 15 is representative of the effects of position/velocity feedback only on the dominant unstable root. A position/velocity gain ratio of 1 was used as the test case.

Feedback stability testing of L_3 in the Heppenheimer model requires two items: One, initial value of feedback gain and two, a reference orbit defined. The most logical initial gain to use is the minimum gain needed to stabilize the Wheeler model; since any gain less than that would also be insufficient to stabilize the Heppenheimer model. This approximate minimum value of gain is read directly from the root locus plots developed above. Next, a reference orbit is required to provide the needed corrections used to stabilize an unstable orbit such as L_3 . Any reference orbit can be used; but to reduce the stabilizing control costs a reference orbit that occurs naturally is desired. Capt. Wiesel (Ref 2) found, as stated earlier, the reference orbit used in this report. He found this orbit by searching for a set of initial

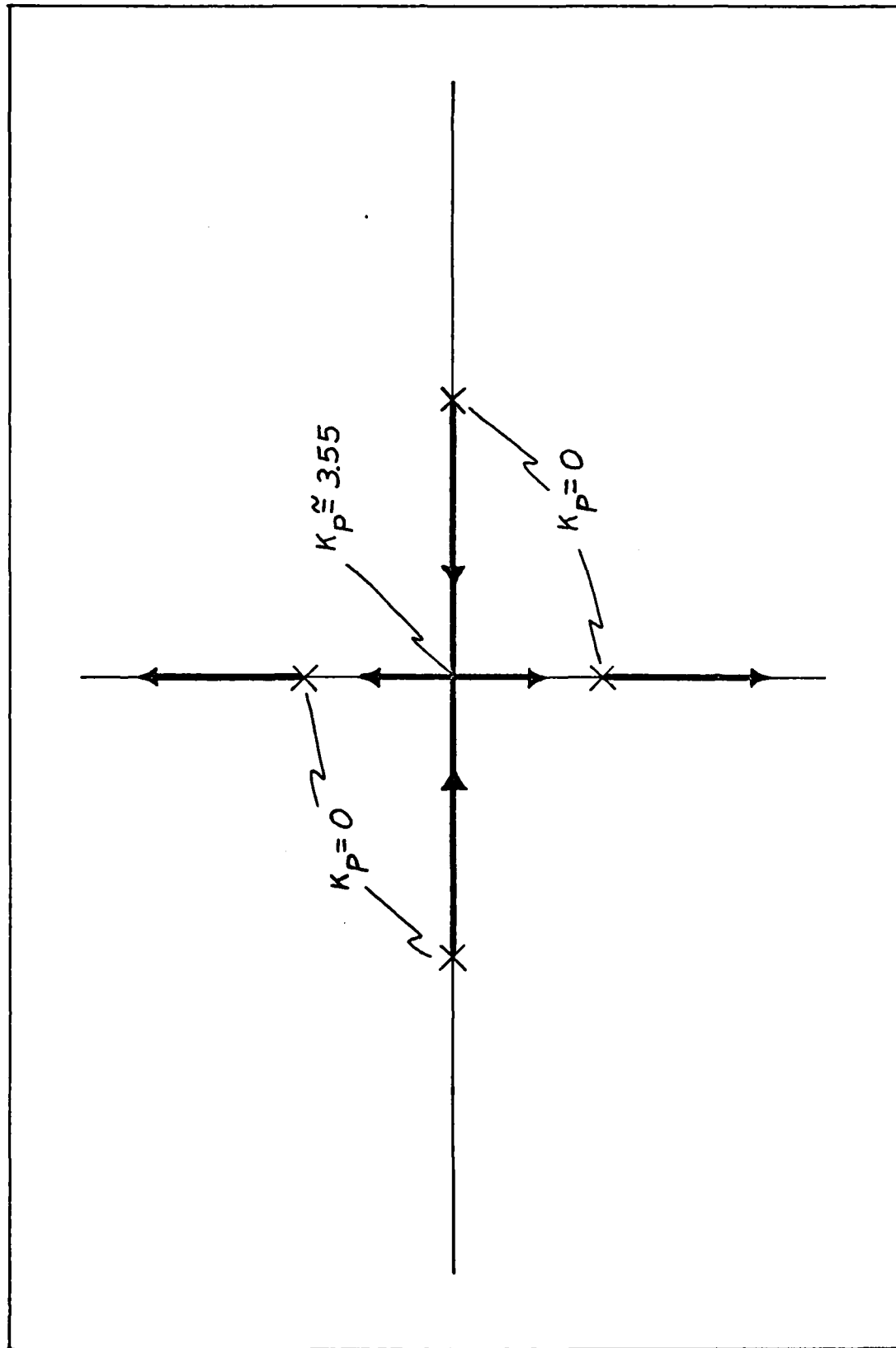


Fig. 13 "Quasi" Root Locus using Position Feedback (schematic)

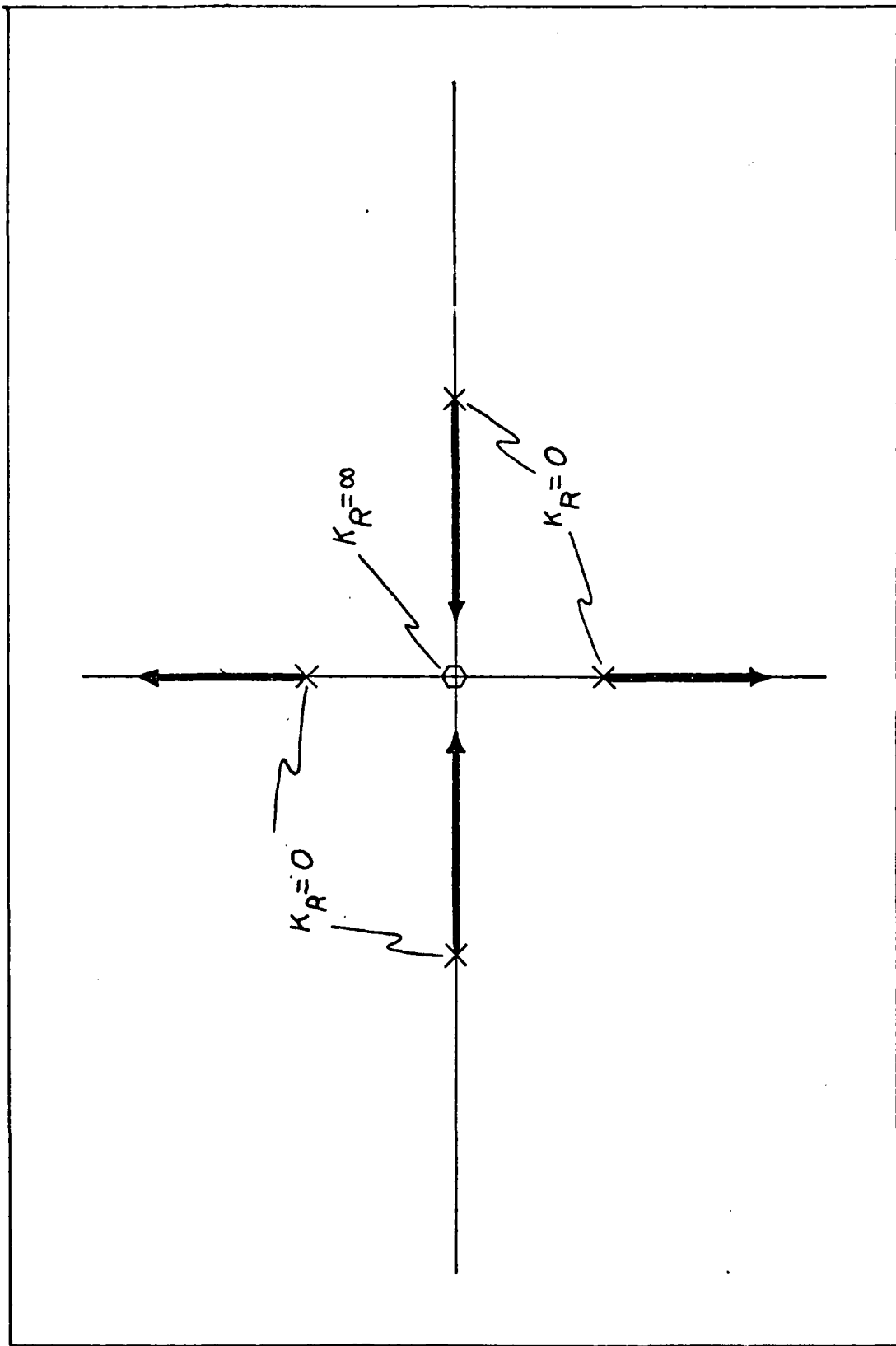


Fig. 14 "Quasi" Root Locus using Velocity Feedback (schematic)

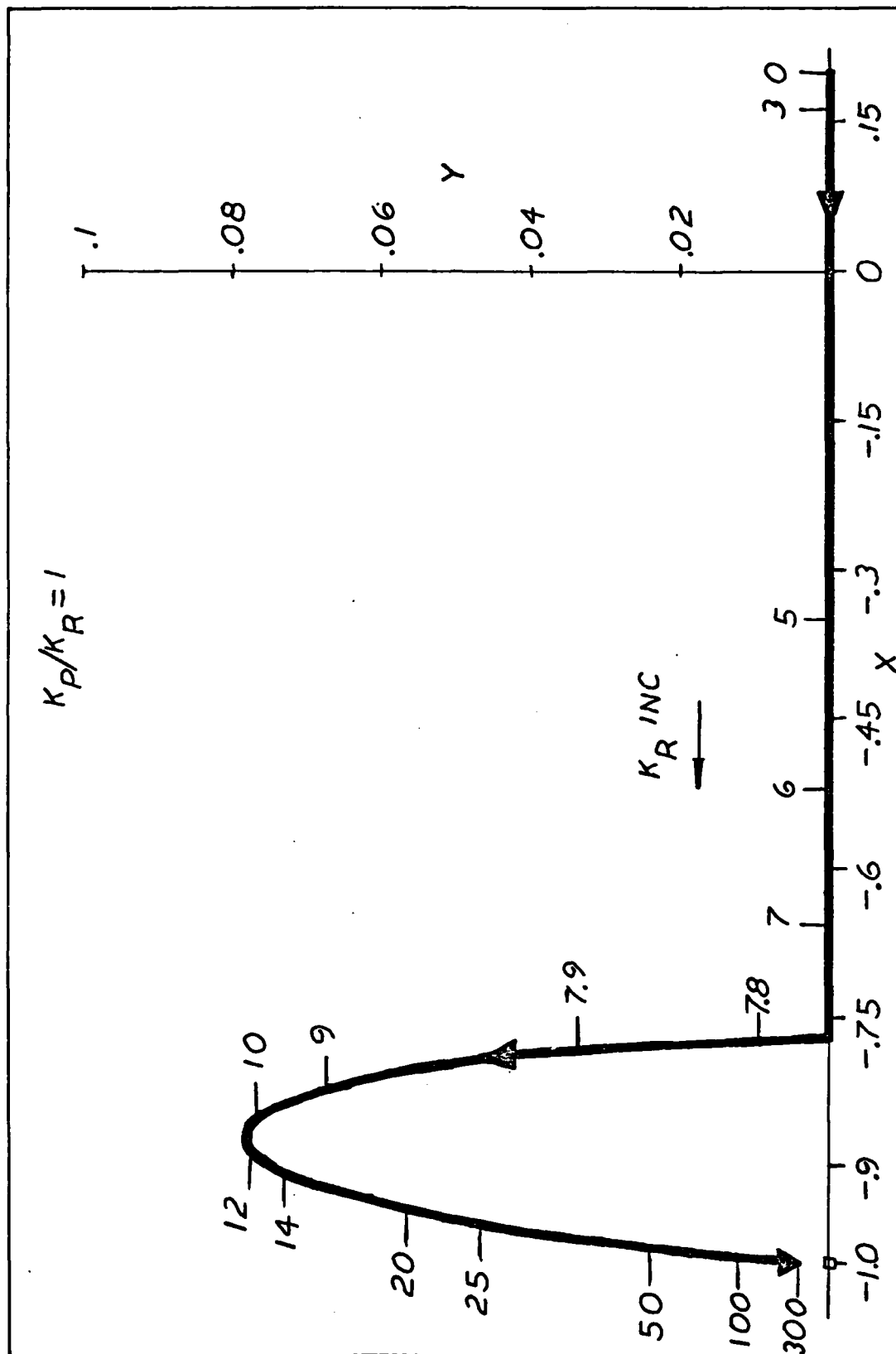


Fig. 15 "Quasi" Root Locus using Position/Velocity Feedback

conditions that would allow an orbit about L_3 to close on itself after one lunar synodic period. Unfortunately, his orbit only closes on itself once, which is indicative of the instability of all orbits about L_3 . Thus, without modification Capt. Wiesel's orbit is unusable as a reference orbit. Since his orbit did close at the end of the first month, that portion can be re-used for each consecutive month as the reference orbit. Re-using Capt. Wiesel's reference orbit as it stands could lead to divergence problems in a long term analysis. To prevent this his periodic one month orbit is expressed in a Fourier series (Ref 8:108) which will always converge as a function of time. The loss of accuracy from using this Fourier series approximation is less than $\pm 1 \times 10^{-10}$. Figures 16 to 21 represent the increased stabilizing effects of position feedback with increasing feedback gain. The reference orbit is included in all figures so that a quantitative assessment of feedback compensation can be made. Figure 22 illustrates the effects of position feedback gain versus integrated control costs.

The use of just velocity feedback compensation was not attempted with any degree of seriousness, because stability in the Wheeler model could not be achieved with velocity feedback. This can be verified by checking the root locus shown in Figure 14. Only in the limit as gain $\rightarrow \infty$ would stability be achieved. However, a few arbitrary values of gain were used to illustrate this fact. These cases are shown in Figures 23 to 25.

Lastly, analysis of position/velocity feedback compensation were run using ratios of position gain (K_p) to velocity gain (K_v) of .05; .5; 1; 10. These choices were somewhat arbitrary, but were picked with some forethought. Ratios .05 and .5 were selected to observe the stability effect of a zero on each side of the dominant stable root. It was theorized that since a zero location close to the dominant root such as .05 and .5 would have little effect on stability; then zeros placed much farther away from the dominant root such as 1 and 10 would have a more profound effect on stability. These effects are presented in Figures 26 to 29.

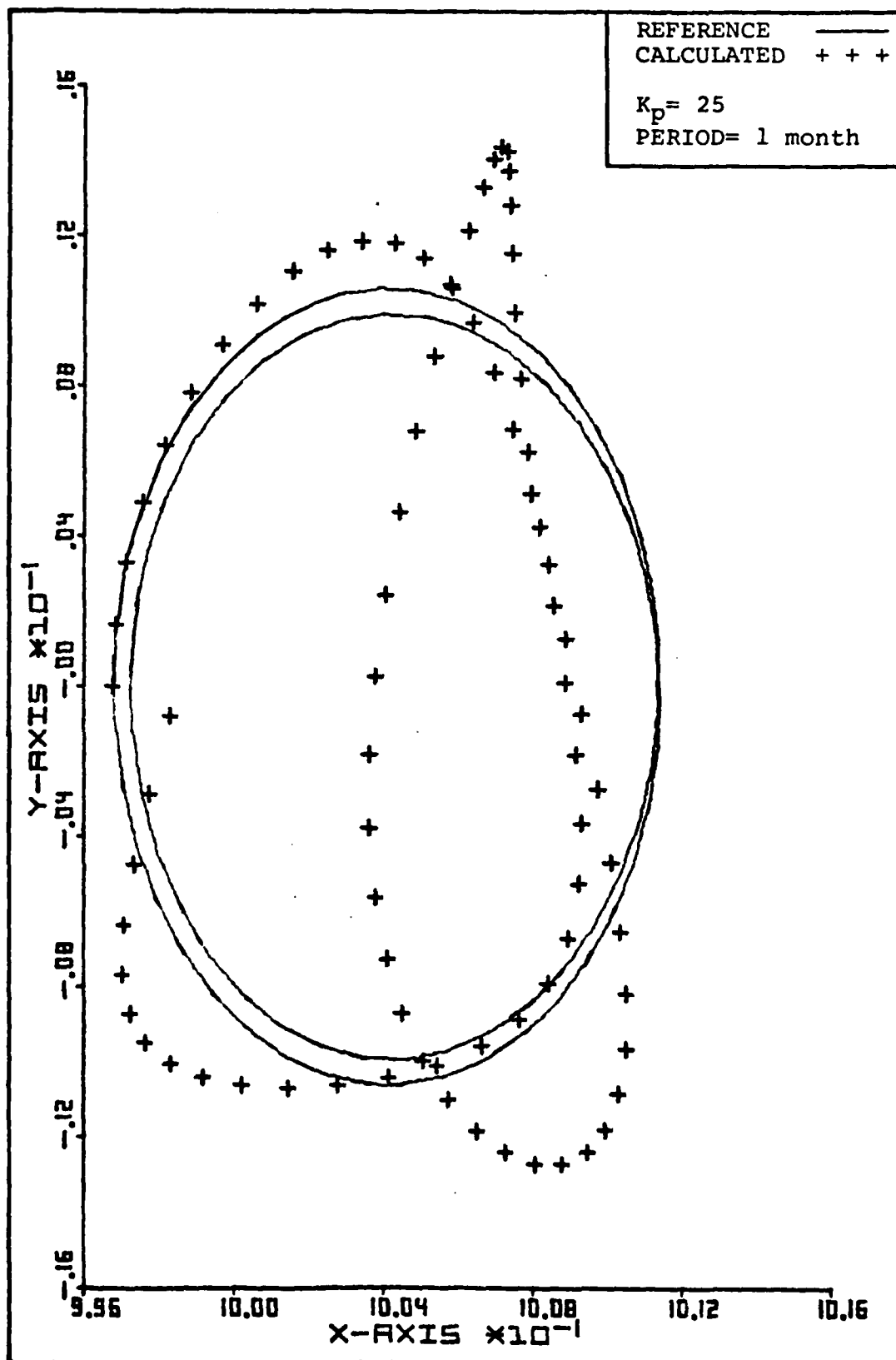


Fig 16. L_3 Orbit using Position Feedback

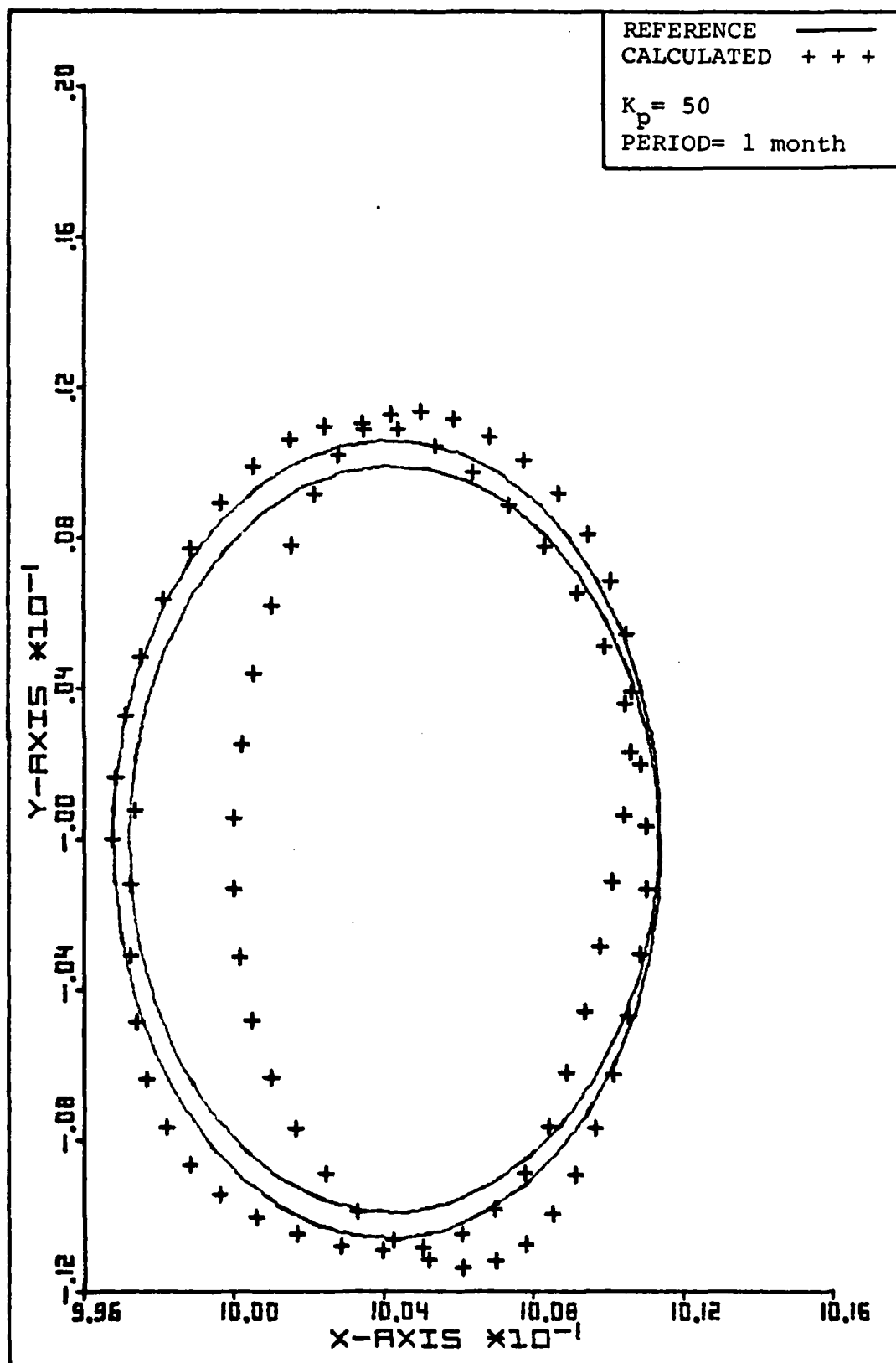


Fig 17. L_3 Orbit using Position Feedback

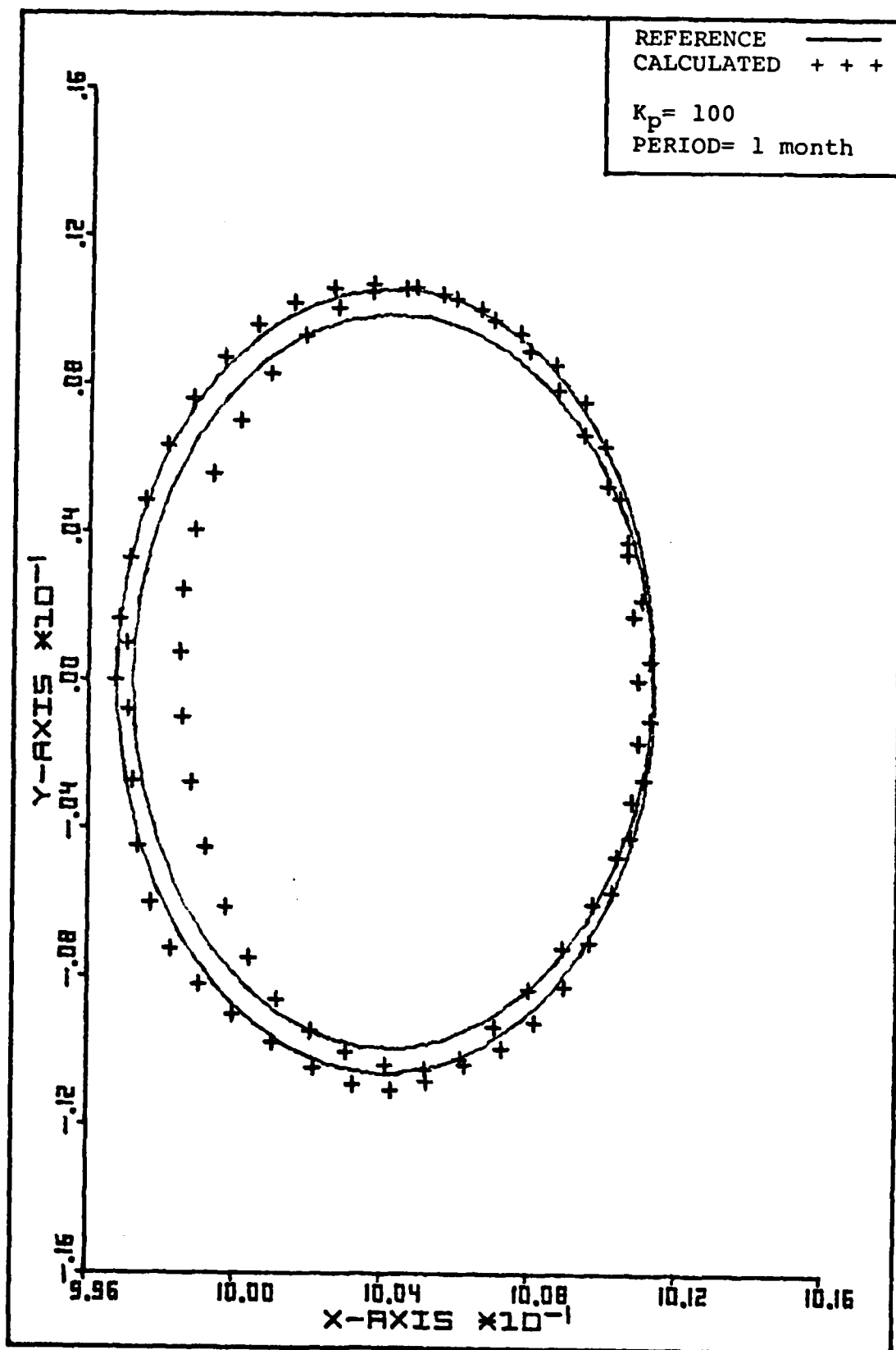


Fig 18. L_3 Orbit using Position Feedback

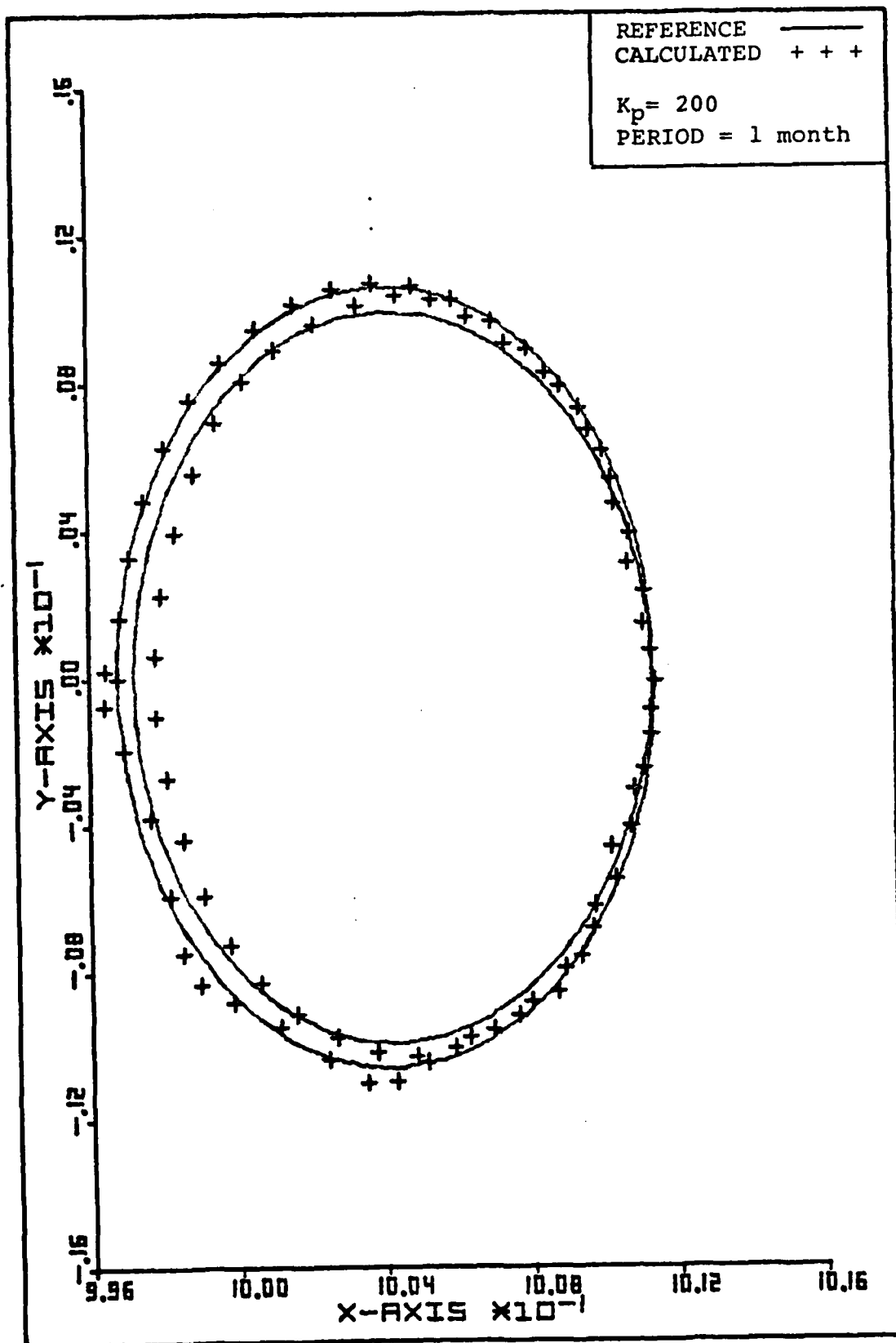


Fig 19. L_3 Orbit using Position Feedback

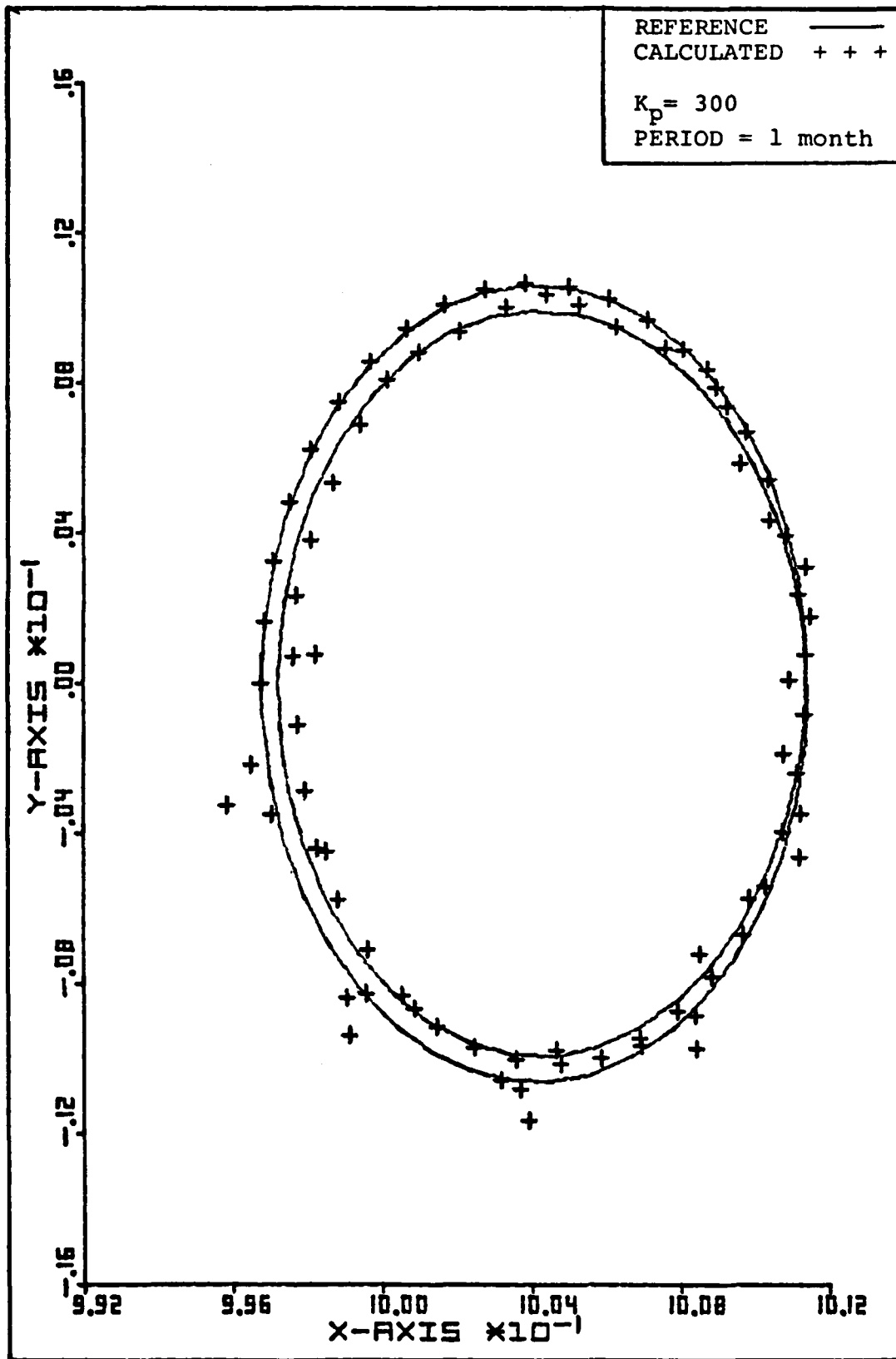


Fig 20. L_3 Orbit using Position Feedback

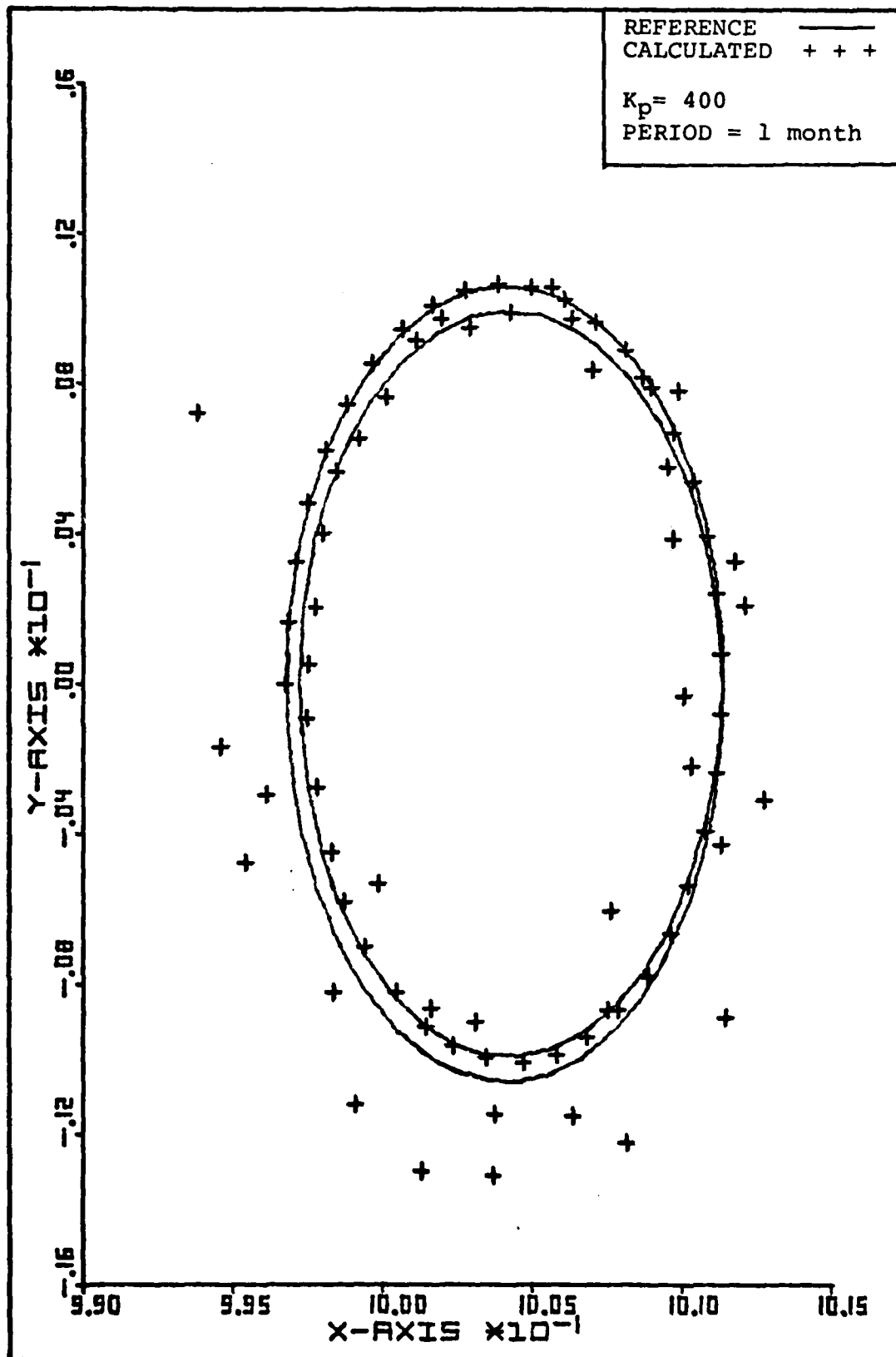


Fig 21. L_3 Orbit using Position Feedback
41

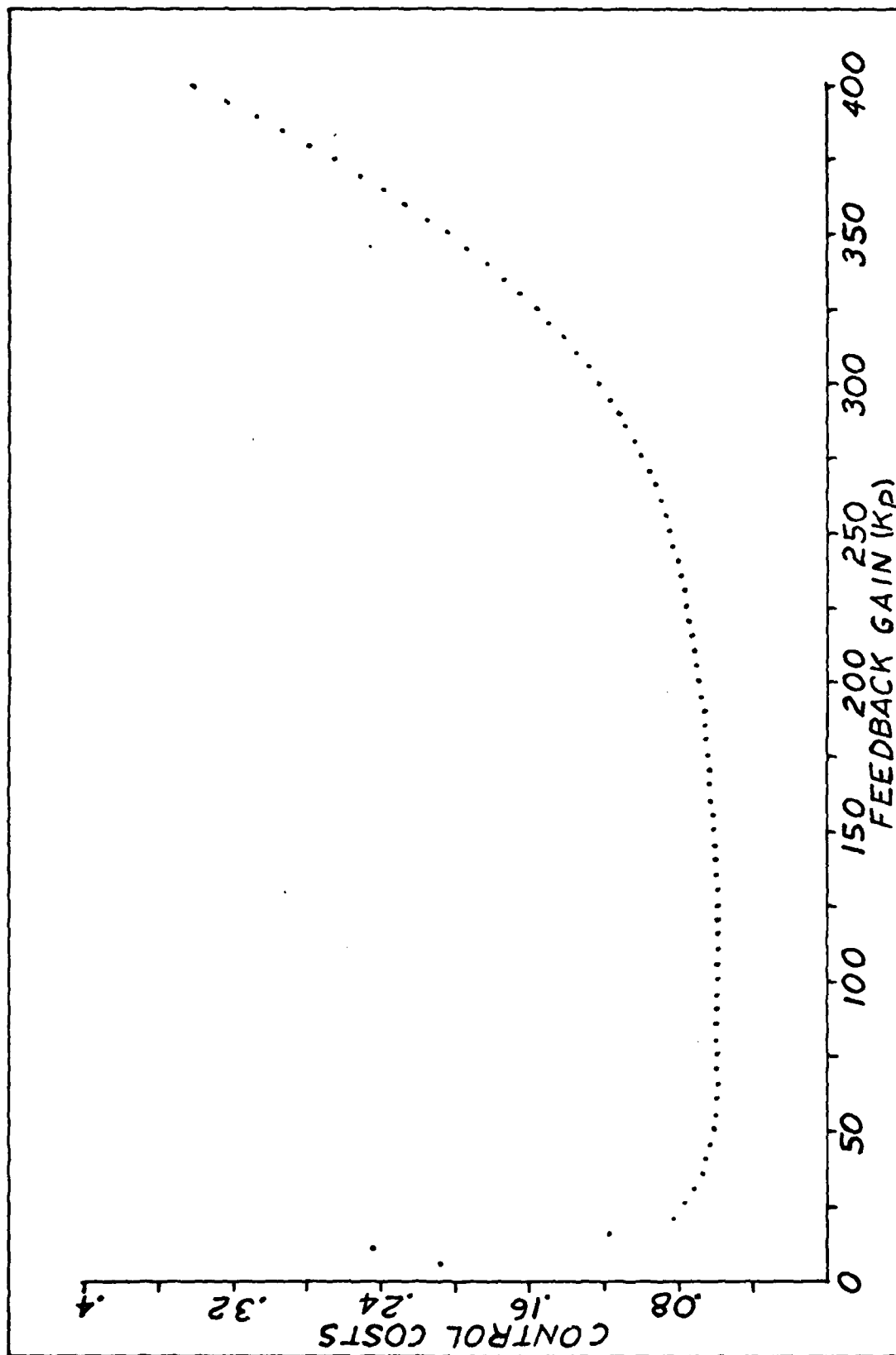


Fig 22. Position Feedback Gain vs Integrated Control Costs

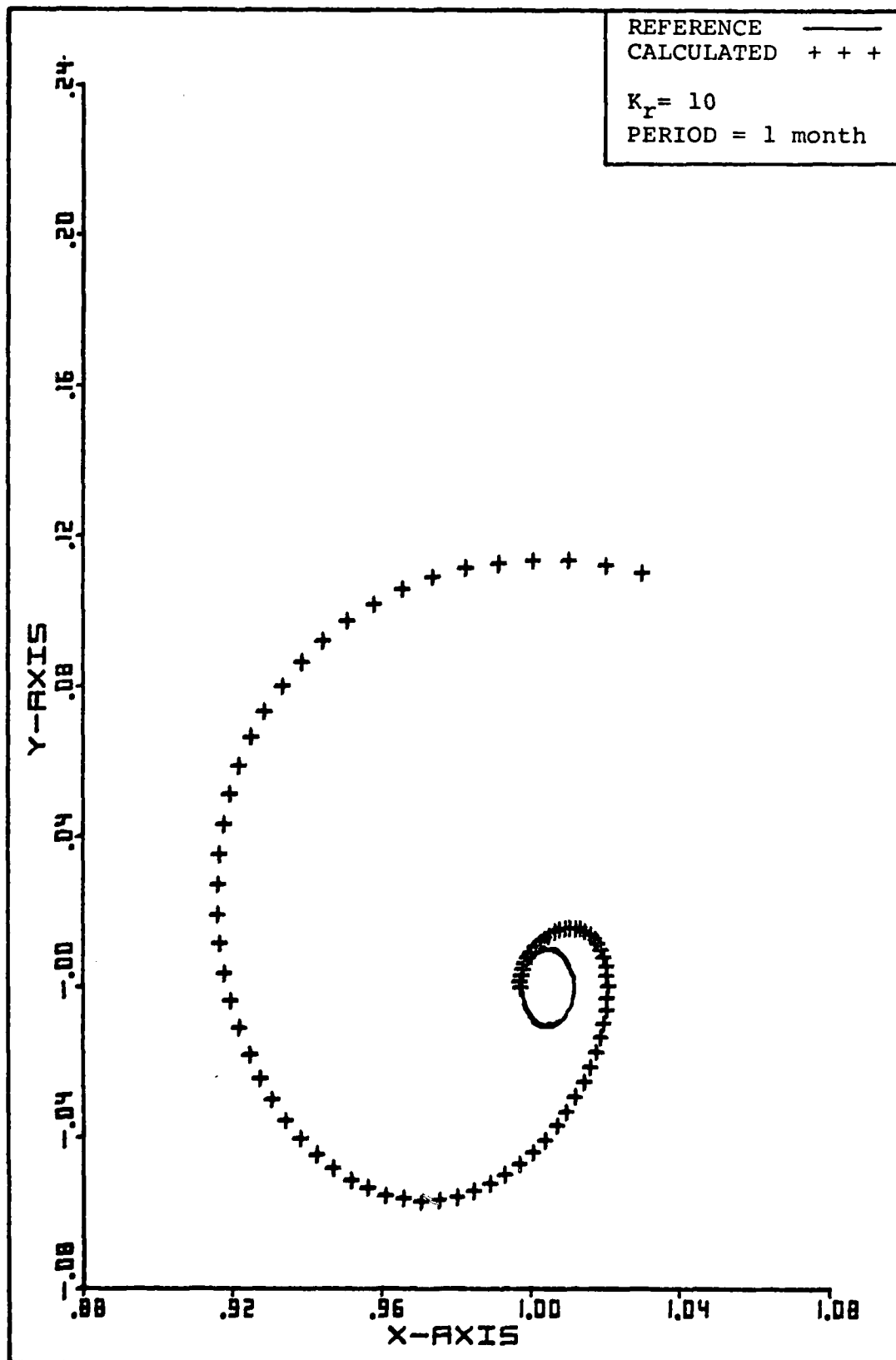


Fig 23. L_3 Orbit using Velocity Feedback

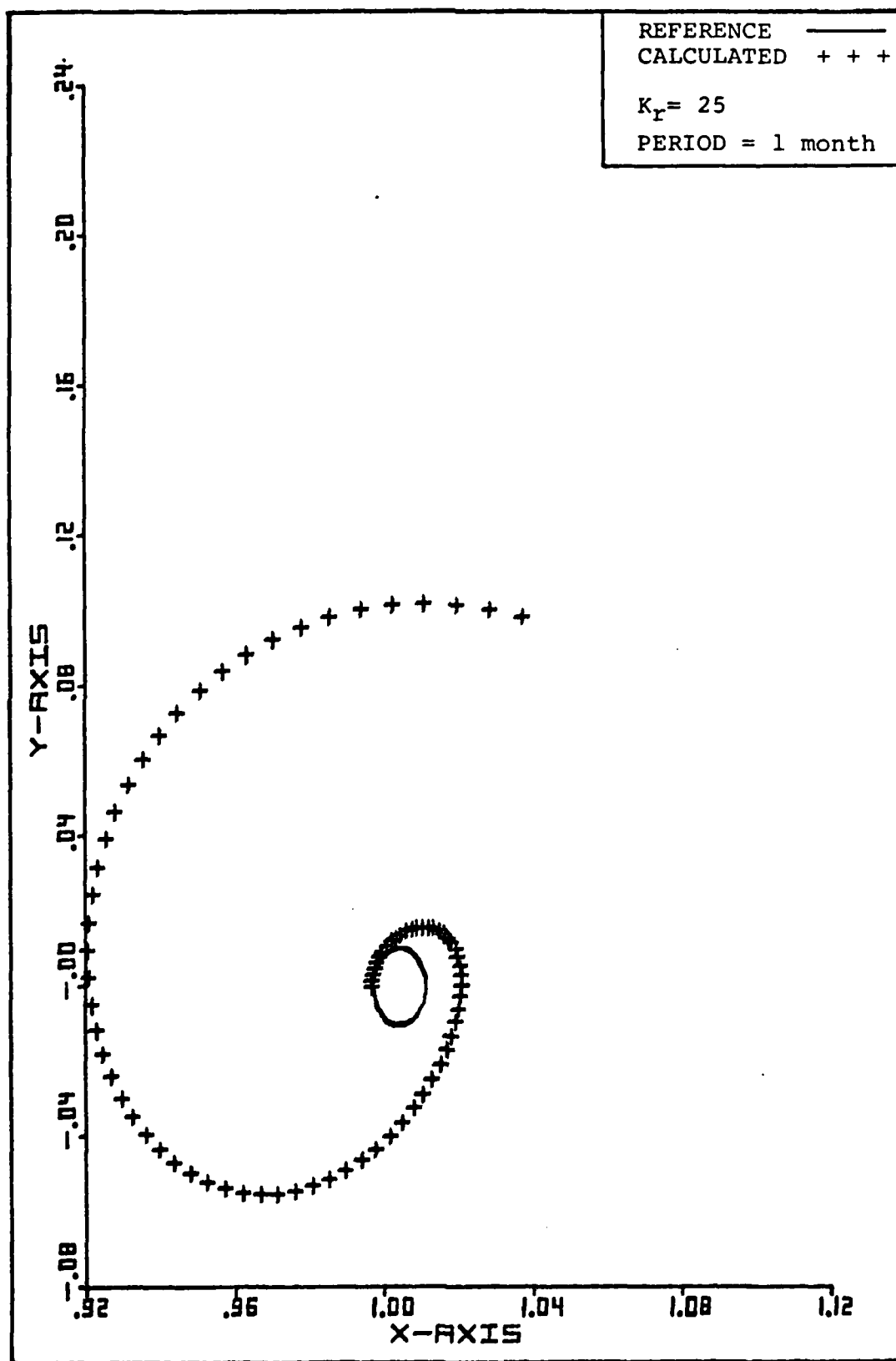


Fig 24. L_3 Orbit using Velocity Feedback

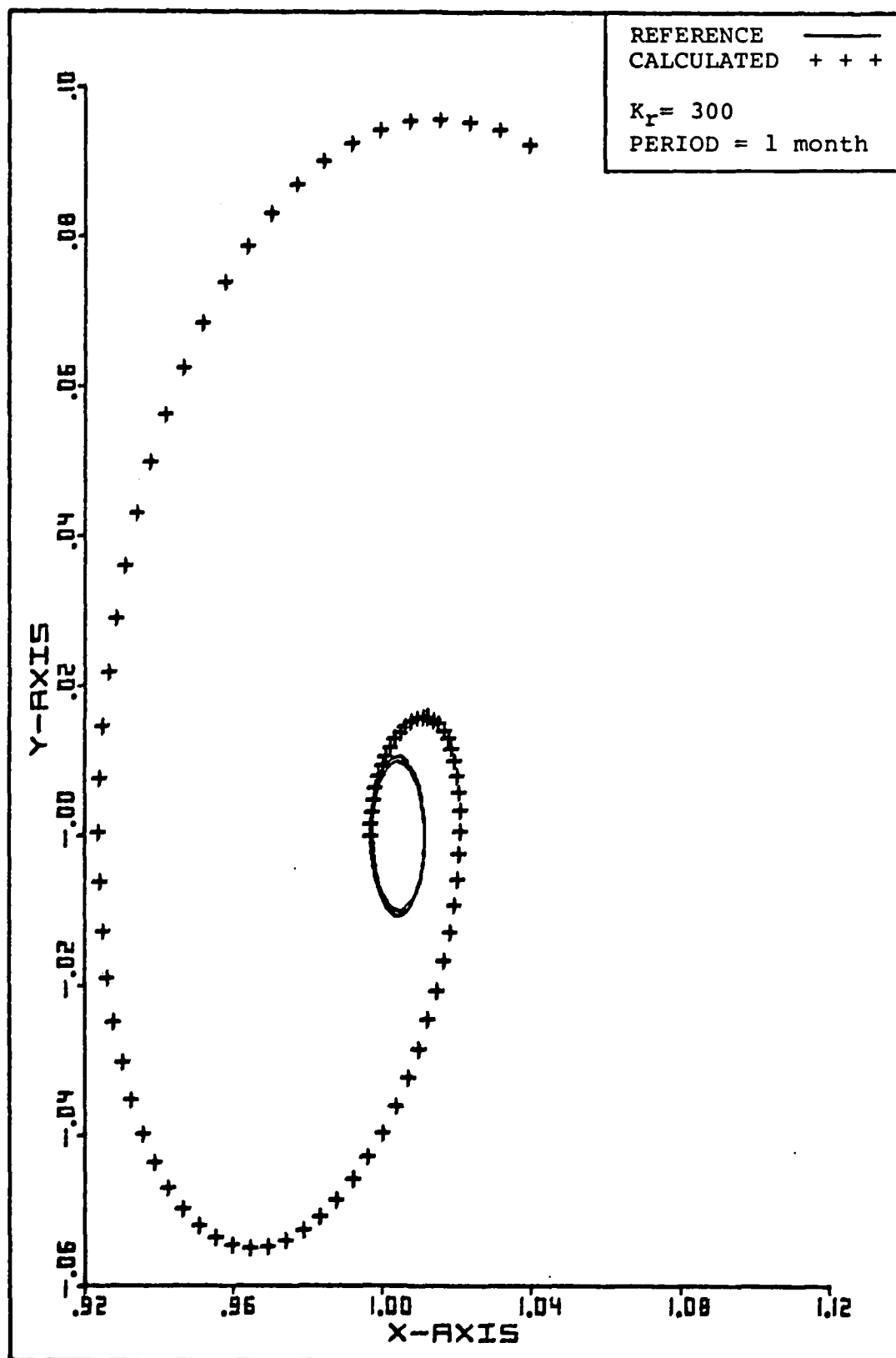


Fig 25. L_3 Orbit using Velocity Feedback

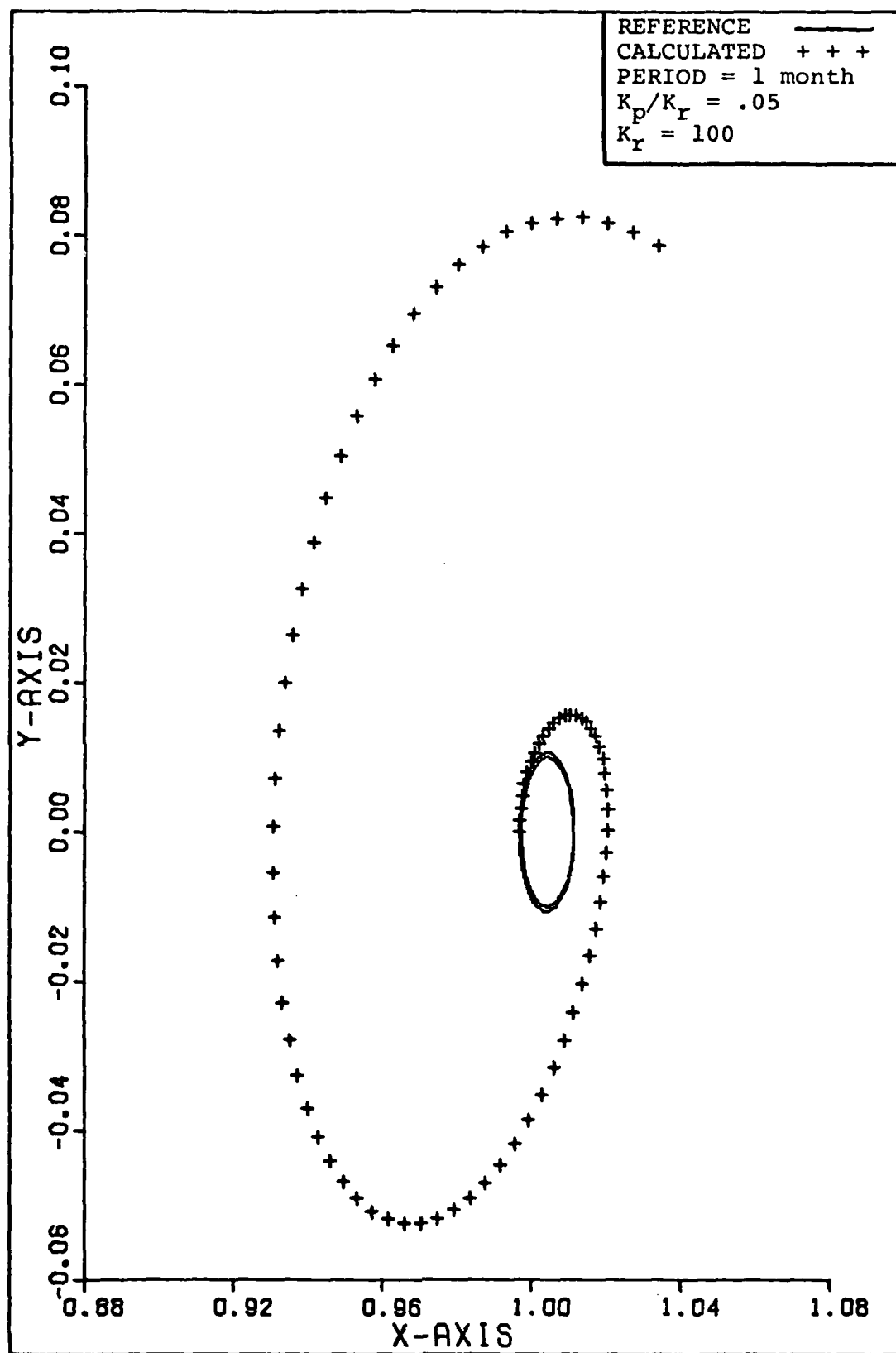


Fig 26. L_3 Orbit using Position/Velocity Feedback

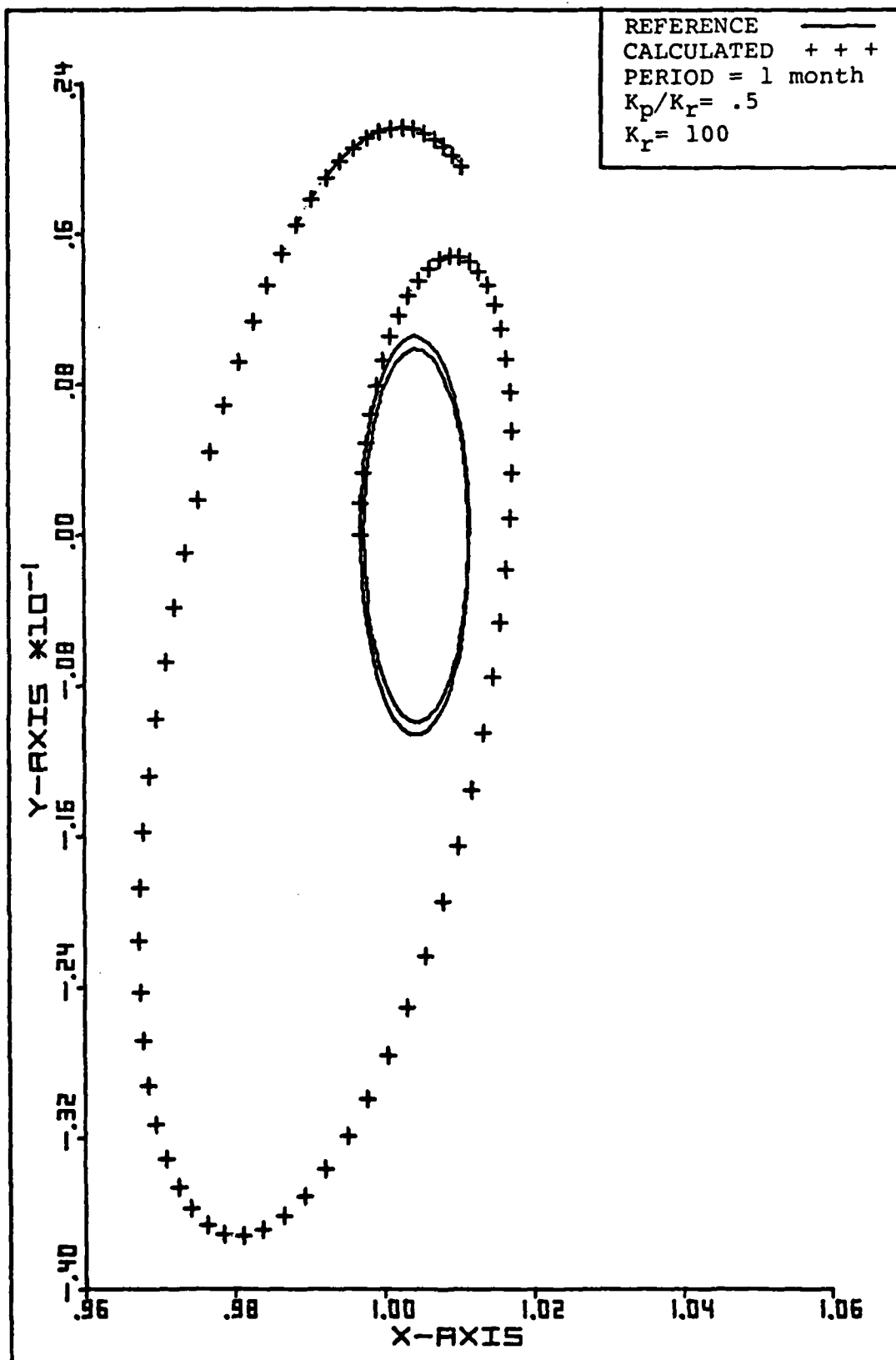


Fig 27. L_3 Orbit using Position/Velocity Feedback

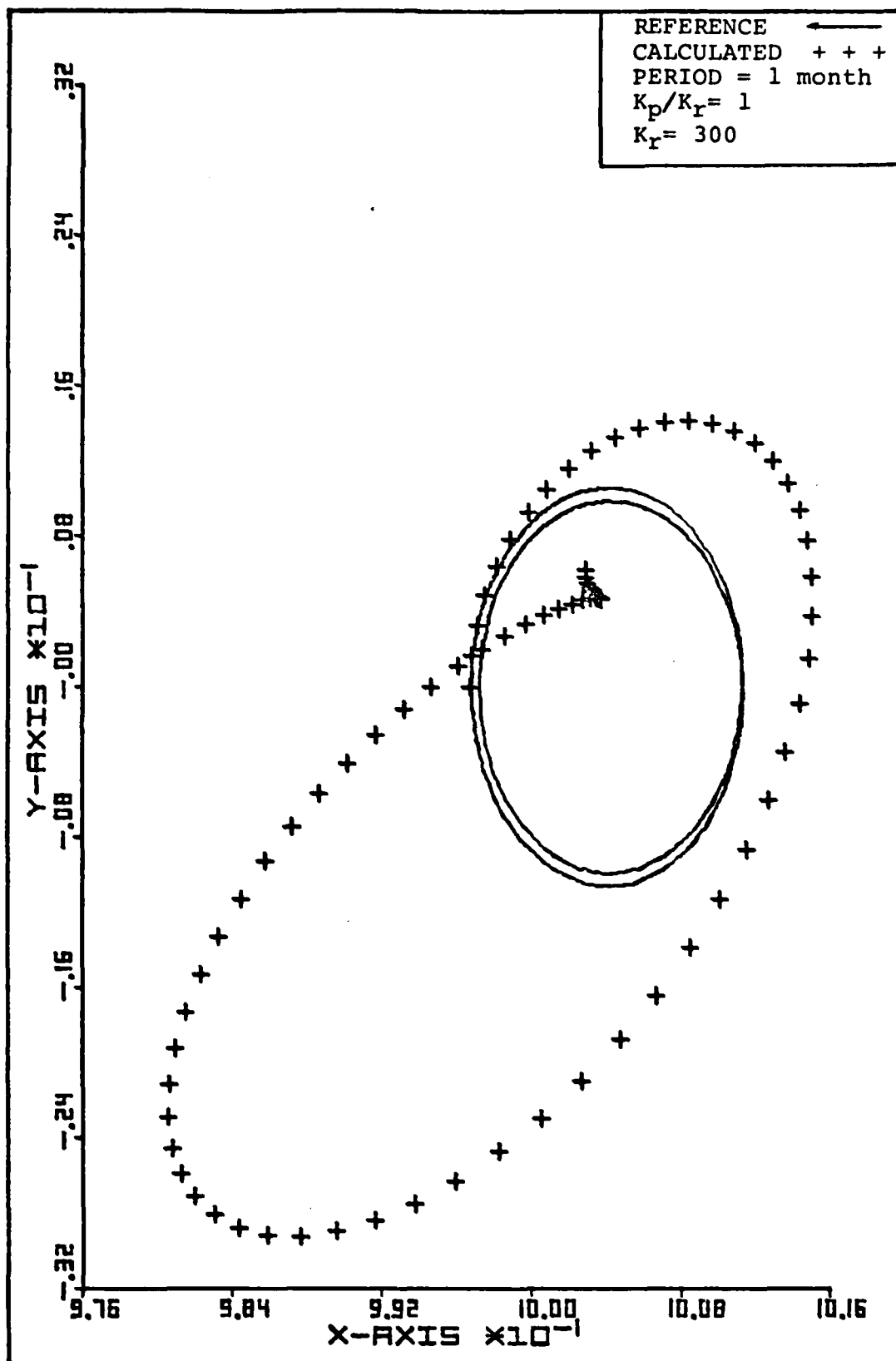


Fig 28. L_3 Orbit using Position/Velocity Feedback

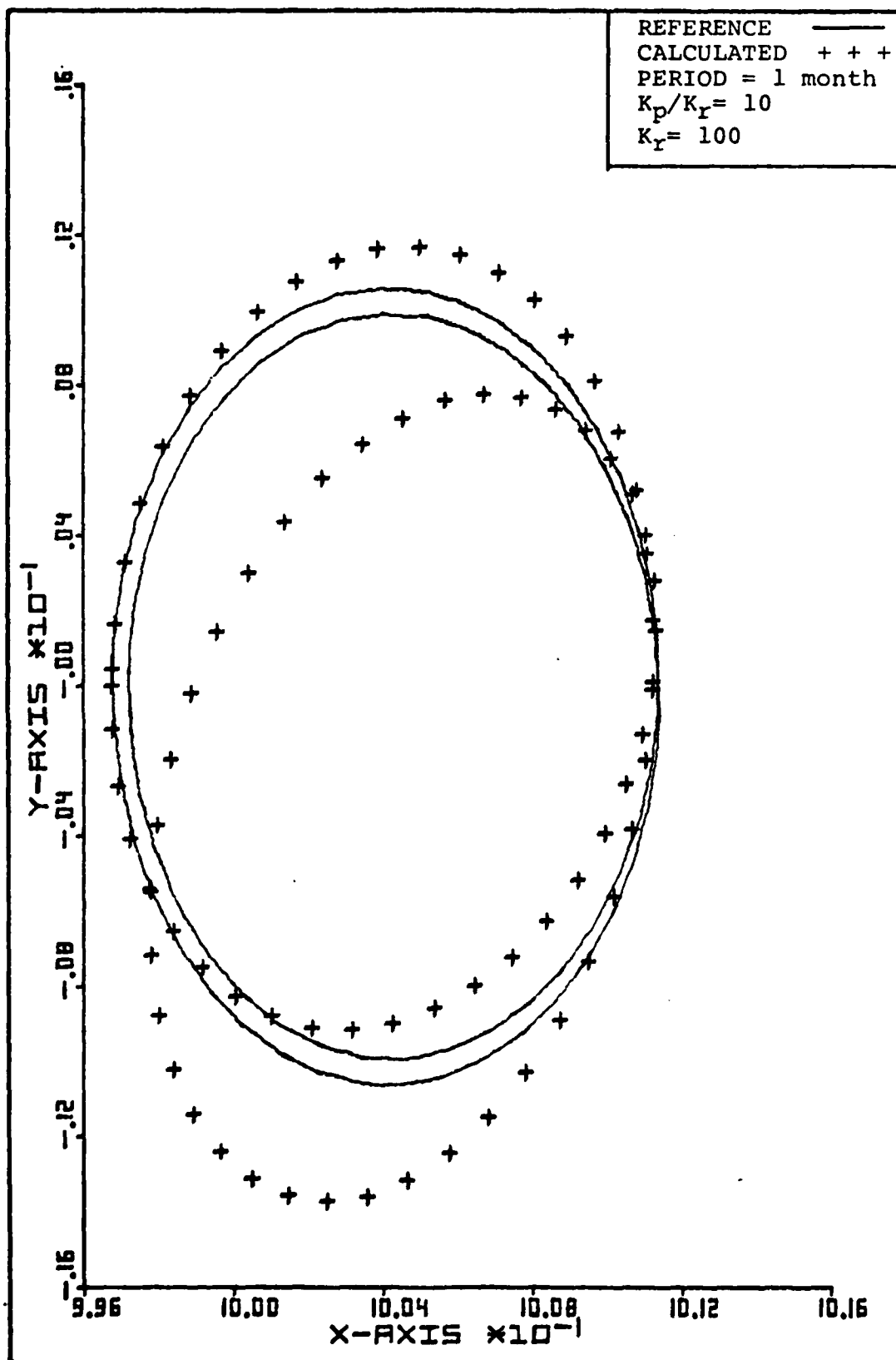


Fig 29. L_3 Orbit using Position/Velocity Feedback

IV. Results and Discussion

Results

A transitory degree of stability was achieved with only position feedback. The duration of stability appeared to be inversely proportional to the amount of gain used. That is, with small values of gain (<150) the calculated orbit would oscillate about the reference orbit with increasingly larger amplitudes until all motion had degenerated into random oscillations. This snowballing effect usually takes two to four months depending upon the gain before completely degenerate motion occurs. Accordingly, large values of gain (>150) would cause the orbit to deteriorate to wild oscillations in much less time. These phenomena are illustrated in Figures 30 and 31. Figure 30 is the calculated orbit for two months with feedback gain equal to 125. As can be seen, the orbit is well behaved for approximately three-fourths of the two month period. However, during the last one-fourth of its period, the orbit begins to degenerate into a spiral or rosette pattern that grows in amplitude with time. Figure 31 represents the same orbit, but with feedback gain equal to 400 and for only one month. Notice again that it has the snowball effect. It is obvious that the orbit has degenerated to wild oscillations in less than one month.

No degree of stability was achieved using only velocity

feedback, as mentioned in Section III. It is felt that the system zero from using velocity feedback effectively blocked the unstable root from migrating to the stable left-half plane. Since that root remains in the right-half plane, the system is always unstable regardless of the magnitude of velocity feedback gain used. Figures 23 to 25 verify the ineffectiveness of velocity feedback.

Position/velocity feedback did create the greatest degree of orbital stability, but not as was originally anticipated. Gain ratios of .05 and .5 were completely ineffective in producing any noticeable degree of stability. This is in line with the behavior predicted in Section III and verified in Figures 26 and 27. Earlier it was felt that moving the zero location farther away from the dominant root would provide a much greater degree of system response to feedback control. However, gain ratios of 1 and 10 were only marginally effective. This was not an expected result. Figure 28 shows the marginal effect of a system zero located at 1. For gain ratio $K_p/K_r = 1$, values of K_r up to 300 were tried. The results were all similar to those depicted in Figure 28.

Control gain costs for $K_p/K_r = 1$ ranged from .04251 for $K_r = 1$ to 8.8765 with $K_r = 300$. This translates into an approximate range of ΔV of 43.4 m/s to 9071.8 m/s. For gain ratio $K_p/K_r = 10$, the effects of K_r between 1 and 100 were tried. The only noticeable effect of increasing K_r was the increase in control gain costs. They are .17676 with $K_r = 1$ to 3.8497 with $K_r = 100$. Correspondingly, the ΔV range is 180.6 m/s to

3934.4 m/s. Comparing Figures 26, 27, 28 and 29 clearly showed that a zero location at 10 provided a more stable orbit than was achieved with zeros at 1 or even .05 and .5, but not nearly what was expected. In a final effort to achieve a more respectable stabilized orbit gain ratio $K_p/K_r = 100$ was tried. This did bring about a dramatic increase in orbital stability. Figures 32 to 34 show the effectiveness of this gain ratio. With $K_r = 10$, this seemed to be the minimum value that brought about the desired degree of stability. $K_r = 100$ also achieved the same degree of stability, but with an order of magnitude increase in control gain costs. Control costs increased from .08032 with $K_r = 1$ to 3.8992 with $K_r = 100$. Again, the ΔV range is 82.1 m/s to 3984.9 m/s.

Comparing control costs for zero locations at 1, 10 and 100 with $K_r = 10$ versus the visual degree of stability shows the calculated orbit zeros in on the reference orbit with an increase in gain ratio while the respective control costs are .30, .39 and .4. The better zero location, as far as stability is concerned, is 100. However, in terms of cost, zero location at 1 is the better location. Within the constraints of the intuitive optimization scheme presented earlier, the zero location at 100 is the desired location.

Discussion

Position feedback can be thought of as adding a spring force in a simple harmonic oscillator. The spring would apply a constant restoring force proportional to the displacement

from a reference position, where the proportionality constant is the spring constant, or in this case the feedback gain. Thus, any orbital position error will generate a restoring force opposing the position error. In essence, this type of control over corrects for any error, i.e. the larger the position error the larger the correction force. Since this system has two oscillatory modes, one stable and one unstable, each position error will have a component from both modes. Therefore, part of the restoring force goes into suppressing the unstable mode; and the remainder contributes to the stable oscillatory mode. Exciting the oscillatory mode creates a larger displacement than the reference orbit predicts, and this produces a position error in addition to the error from the unstable mode. The cumulative effect from exciting the stable oscillatory mode is the mechanism that creates the snowball effect to system instability seen in Figures 30 and 31.

Velocity feedback is normally used to introduce damping into a system. The net result of damping as time $(t) \rightarrow \infty$ reduces the amplitude of the oscillatory mode to 0. This damping effect is caused by introducing a zero into the system's transfer function. Relating to this report, constant gain velocity feedback introduced a zero at the origin of the system's root locus. This has two effects: First, it decreases the amplitude of the oscillatory mode. Second, it keeps the unstable root in the right-half plane. Since the unstable root is kept in the right-half plane, divergent or

unstable motion occurs. With increasing gain the amplitude does decrease due to the damping effect of velocity feedback, but the divergent spiral due to the unstable root is still quite evident.

Using both position and velocity feedback brought about the desired motion. The effect of larger gain ratios was to increase system response to feedback control. Gain ratios of .05 and .5 did little to aid in system stability, because the damping effect is so small. Gain ratios of 1 and 10 increased the sensitivity of the system to feedback control but not to a desired level. With the gain ratio at 100, the system response has been enhanced to the point where position/velocity feedback are effective feedback control elements.

This report did not utilize any sophisticated feedback networks. This simplistic approach to orbital stability was to show that an orbit about L_3 could be stabilized and what it might cost in terms of an approximate ΔV required. Although stability could be achieved, more sophisticated approaches could be used with a larger degree of effectiveness. Two of these approaches would be modal control and lead/lag compensation. As a result of this analysis, modal control appears to be the most logical and easiest to implement. Since only one of the two modes of this system is unstable, applying control to that mode and eliminating the control from the oscillatory mode should be a more economical approach. This would reduce the modal feedback coupling and eliminate the snowball effect found in this report. Using

lead/lag compensation with velocity feedback would allow placement of a zero at a more optimal location other than at the origin of the root locus. Hence, a greater degree of flexibility to system design would be possible. Correspondingly, control gain costs can be minimized.

This report also neglected the effects of orbit plane inclination, planetary perturbations and other minute forces such as solar wind, radiation pressure, etc. The most important of these neglected perturbations is orbit plane inclination. Since planar motion was assumed throughout this report, this major secondary perturbation was neglected. The effect of orbit inclination is to introduce non-planar motion. The long term cumulative effect of this unaccounted for motion might be very detrimental to an orbit as sensitive to disturbing forces as L_3 , even though out of plane forces always tend to return the satellite to the orbit plane.

In this model the control used requires continuous knowledge of the position and velocity states. Laser or radar ranging might be a method of providing the control system with this information. Further consideration of measuring the states beyond mentioning these feasible methods was not considered.

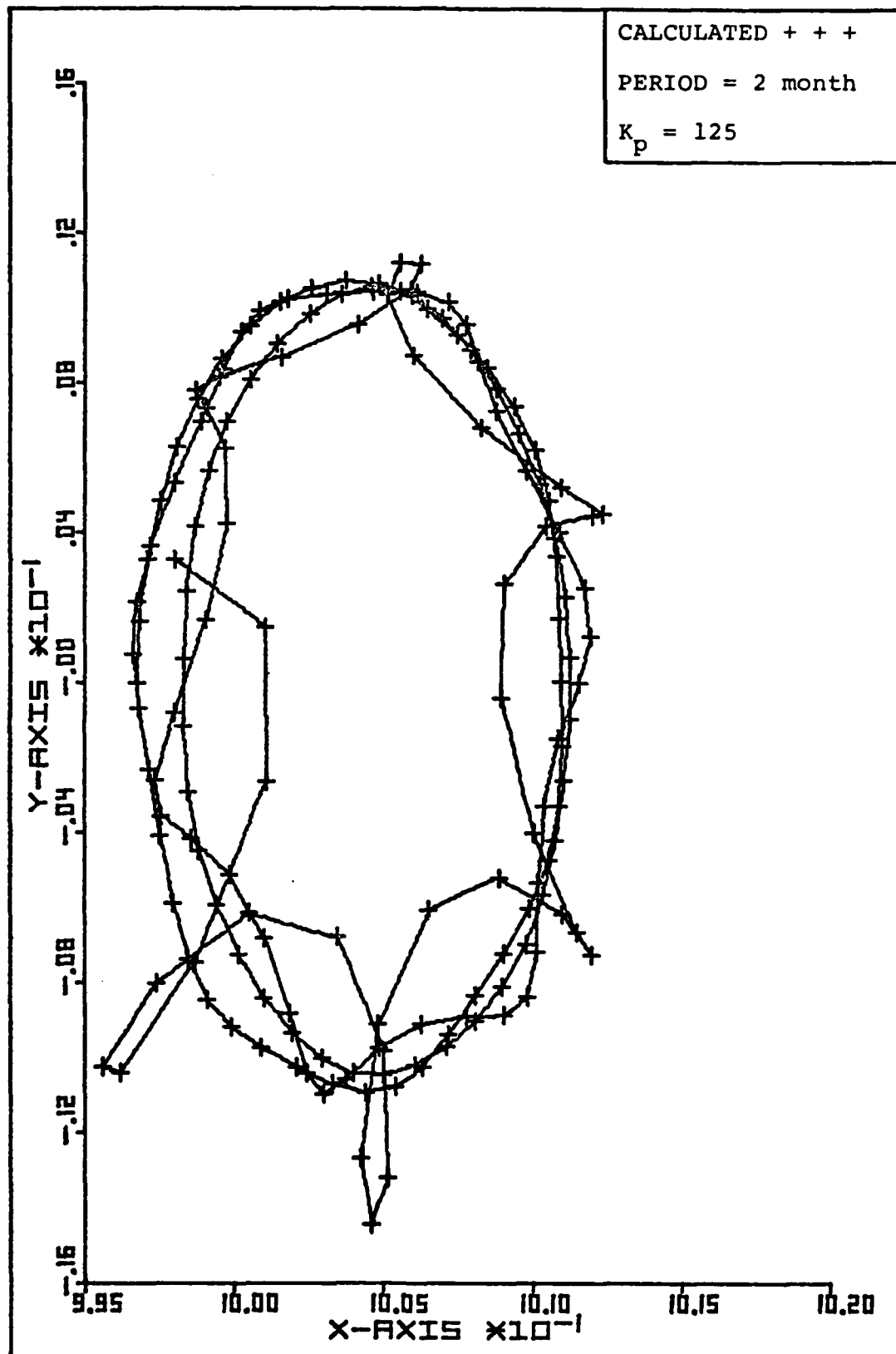


Fig 30. L_3 Orbit using Position Feedback

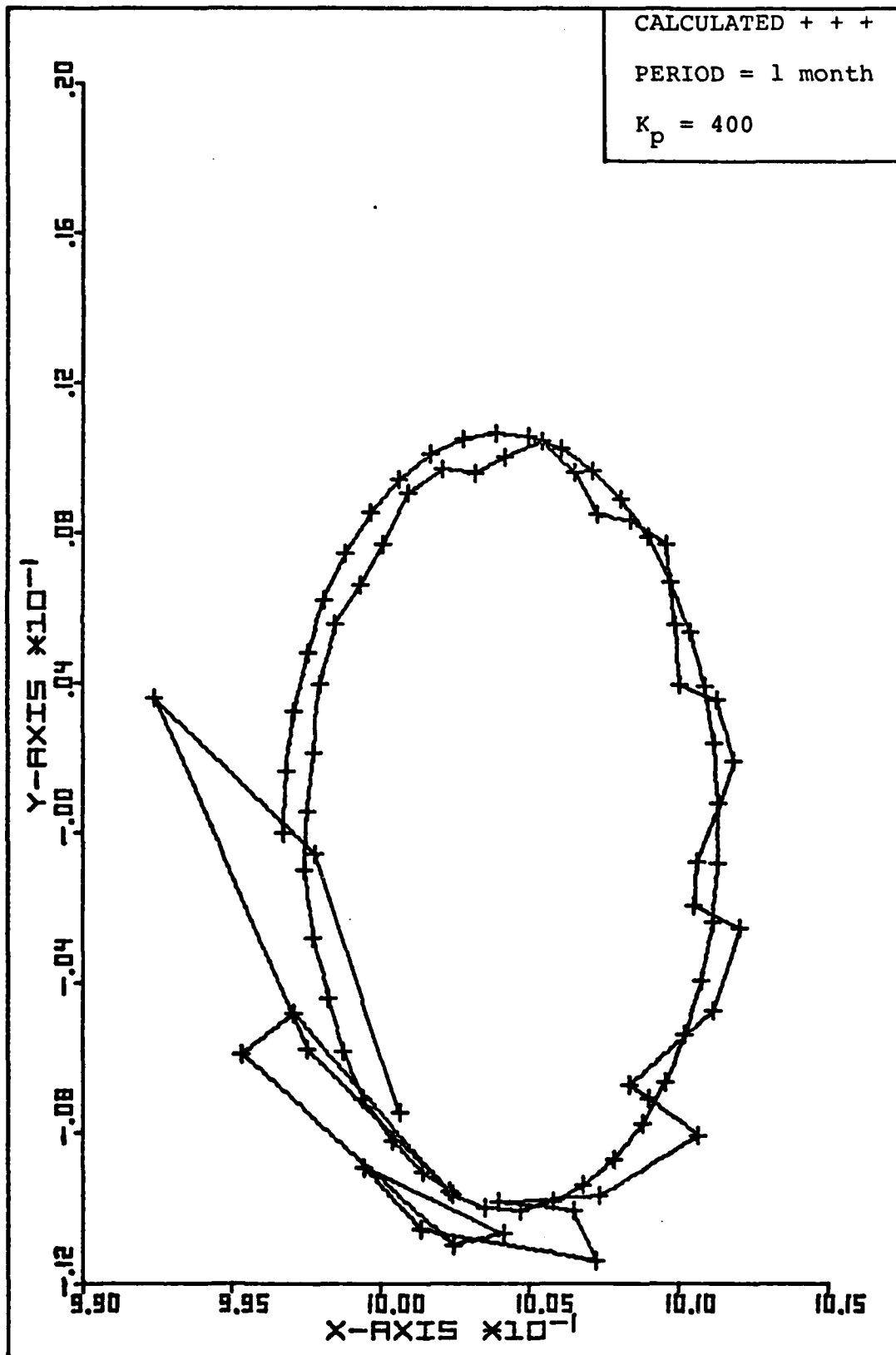


Fig 31. L_3 Orbit using Position Feedback

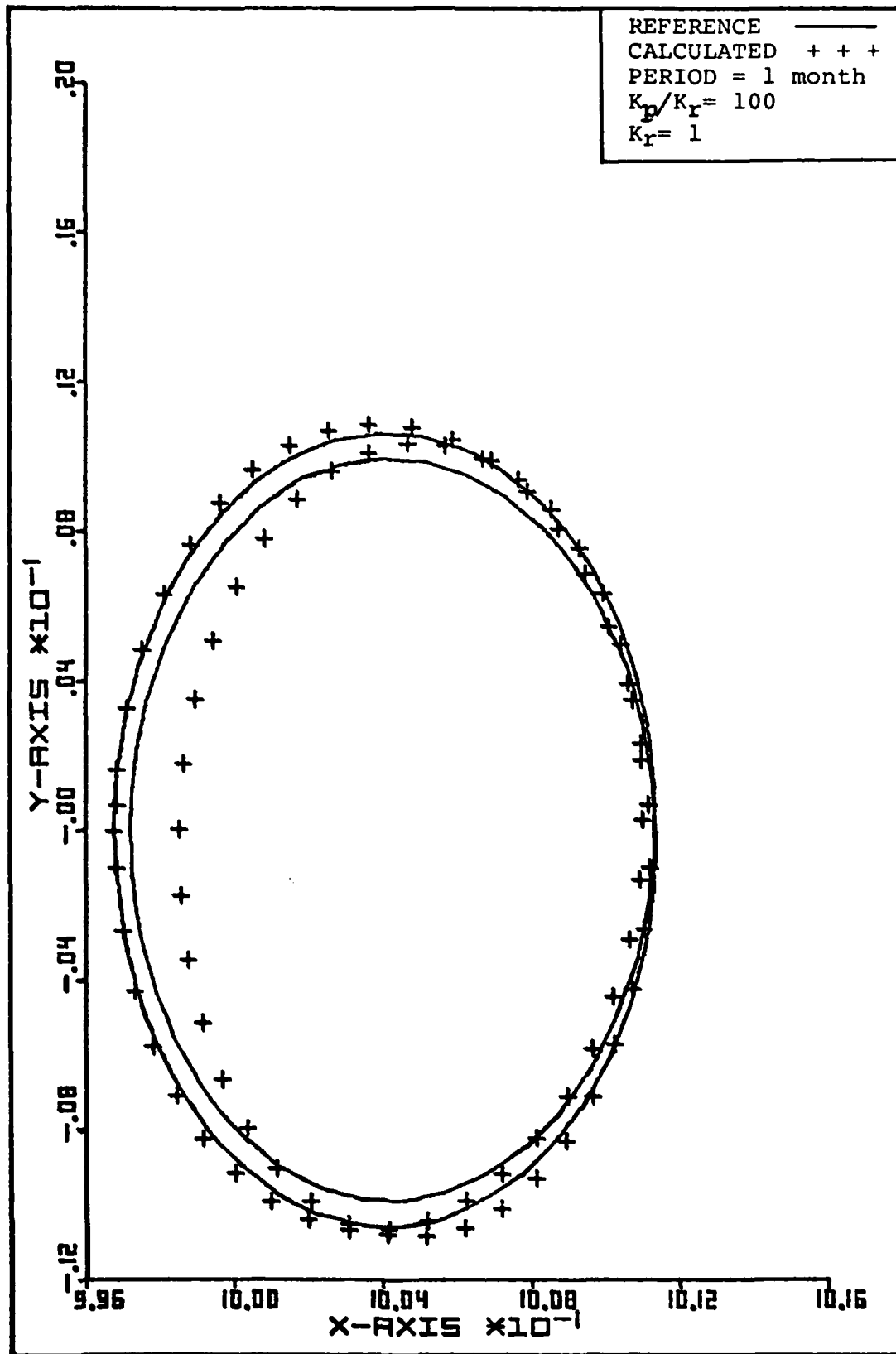


Fig 32. L_3 Orbit using Position/Velocity Feedback

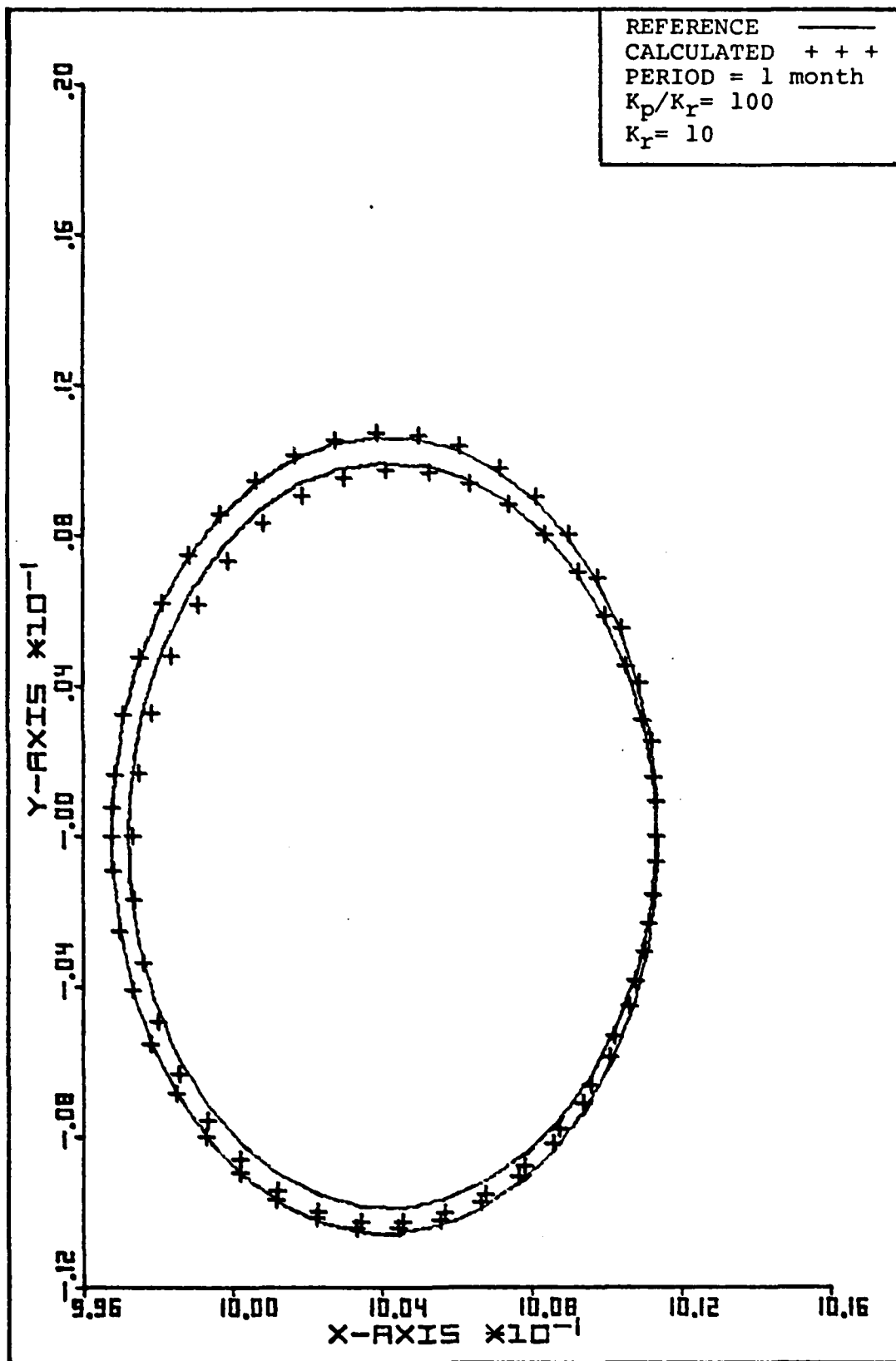


Fig 33. L_3 Orbit using Position/Velocity Feedback

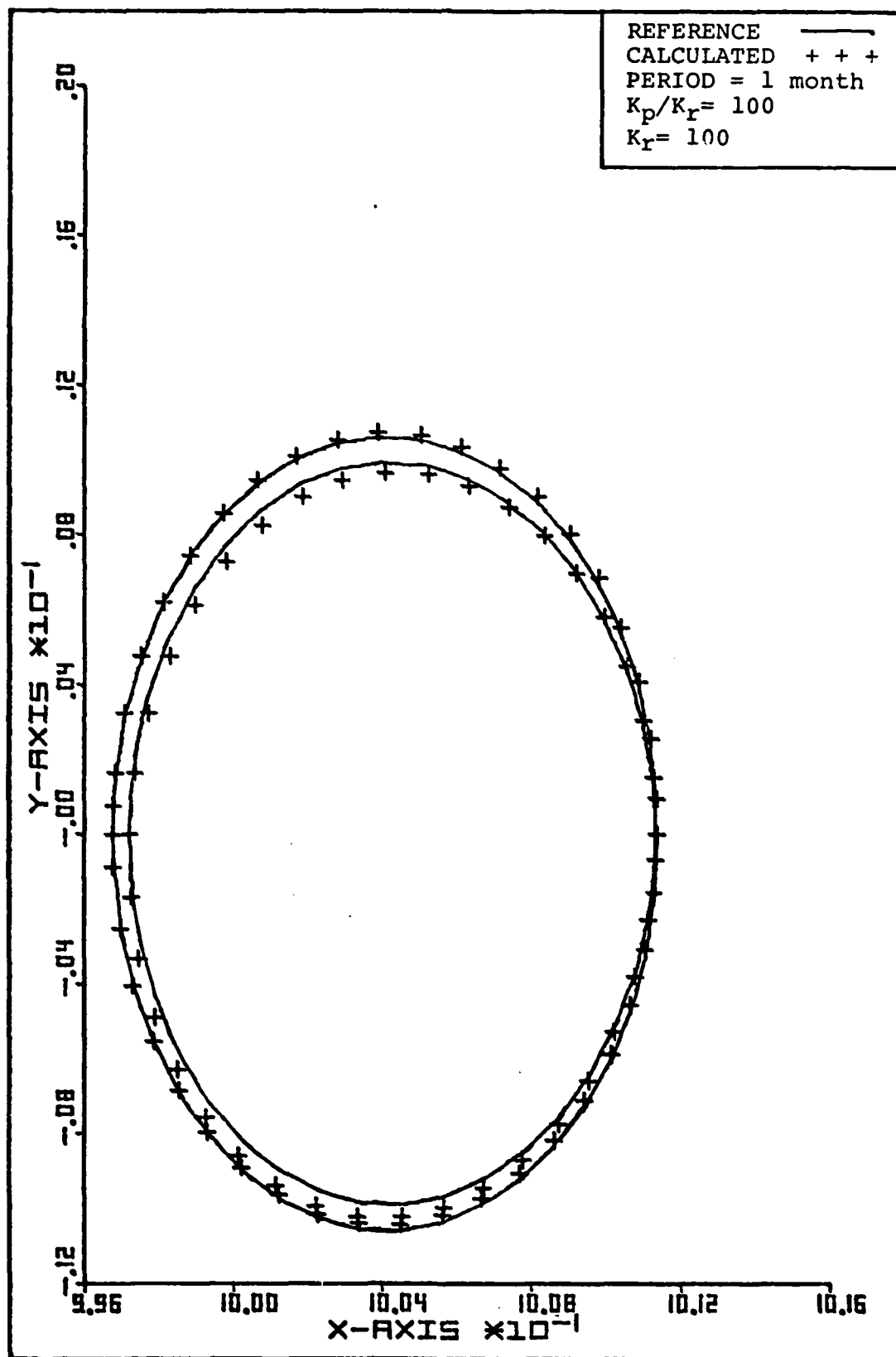


Fig 34. L_3 Orbit using Position/Velocity Feedback

V. Summary and Recommendations

Summary

Using the Wheeler model as an approximate solution to the reduced Heppenheimer model significantly reduced the amount of trial and error testing that would have been otherwise necessary. Analysis of the Poincaré exponents, provided by the Wheeler model, simplified the task of choosing the amount of feedback gain to use. Long term stable motion near libration point L_3 could only be achieved with position/velocity feedback. The associated control gain costs indicate this is not an economical method for stabilization. The Heppenheimer model is an accurate model for studying orbital motion near libration points.

Recommendations

Since a periodic orbit about L_3 has been discovered and it has been shown that it can be stabilized; any refinements to the reference orbit and method of stabilization would be natural follow-on topics. The most logical topic would be a more sophisticated feedback controller. The idea of modal control, mentioned earlier, needs to be examined in detail. Lead/lag compensation could offer attractive stabilizing benefits without a correspondingly large increase in control costs. Also, a three dimensional stability analysis about

L_3 which includes the effects of orbit plane inclination should be examined for applicability to a "real world" situation.

Finally, determining whether or not another periodic orbit about L_3 exists which closes on itself more than once, would naturally lead to reduced control gain costs.

Bibliography

1. Wheeler, John E. "Determination of Periodic Orbits and Their Stability in the Very Restricted Four-Body Model in the Vicinity of the Lagrangian Points L_4 and L_5 ." Unpublished thesis. Wright-Patterson Air Force Base, Ohio: Air Force Institute of Technology, December 1978.
2. Wiesel, W. E. Unpublished research notes. Wright-Patterson Air Force Base, Ohio: Air Force Institute of Technology.
3. Berge, T. K. Lunar Libration Points: Their Potential Usefulness. Air War College Report No. 3292. Maxwell Air Force Base, Alabama: Air War College, April, 1967.
4. Heppenheimer, T. A. "Steps Toward Space Colonization: Colony Location and Transfer Trajectories." Journal of Spacecraft and Rockets, 15:305-12 (1978).
5. Danby, J. M. A. Fundamentals of Celestial Mechanics. New York: The Macmillan Company, 1962.
6. Szebehely, V. Theory of Orbits. New York: Academic Press, 1967.
7. Meirovitch, Leonard Methods of Analytical Dynamics. New York: McGraw-Hill Book Company, 1970.
8. Brouwer, D. and Clemence, G. M. Methods of Celestial Mechanics. New York: Academic Press, 1961.
9. Bate, R. B., et al. Fundamentals of Astrodynamics. New York: Dover Publications, Inc., 1971.

Appendix A

Derivation of the Heppenheimer Equations

The equations of motion for this model are given by the vector sum of all gravitational forces acting on that body. Newton's law of universal gravitation is applied to determine those gravitational forces. Newton's law of universal gravitation can be expressed mathematically as

$$\underline{F}_g = - \frac{GM_m}{r^2} \frac{\underline{r}}{r} \quad (\text{A-1})$$

Figure 35 shows the vector diagram of an arbitrary four body system.

From Newton's second law of motion,

$$\ddot{\underline{r}} = \frac{\underline{F}_t}{m_i} - \dot{\underline{r}} \frac{\dot{m}_i}{m_i} \quad (\text{A-2})$$

where \underline{F}_t is the vector sum of all forces. In this model only the gravitational forces are considered.

Applying (A-2) to each of the four bodies in Figure 35 yields the following:

$$\ddot{\underline{r}}_1 = -G \sum_{\substack{j=2 \\ j \neq 1}}^4 \frac{M_j}{r_{j1}^3} \underline{r}_{j1} \quad (\text{A-3})$$

$$\ddot{\underline{r}}_2 = -G \sum_{\substack{j=1 \\ j \neq 2}}^4 \frac{M_j}{r_{j2}^3} \underline{r}_{j2} \quad (\text{A-4})$$

$$\ddot{\underline{r}}_3 = -G \sum_{\substack{j=1 \\ j \neq 3}}^4 \frac{M_j}{r_{j3}^3} \underline{r}_{j3} \quad (\text{A-5})$$

$$\ddot{\underline{r}}_4 = -G \sum_{\substack{j=1 \\ j \neq 4}}^4 \frac{M_j}{r_{j4}^3} \underline{r}_{j4} \quad (\text{A-6})$$

Arbitrarily selecting body 1 as the Earth and body 4 as the satellite, the position vector for the satellite with respect to the Earth is

$$\underline{r}_{14} = \underline{r}_4 - \underline{r}_1 \quad (\text{A-7})$$

Taking two time derivatives yields

$$\ddot{\underline{r}}_{14} = \ddot{\underline{r}}_4 - \ddot{\underline{r}}_1 \quad (\text{A-8})$$

Substituting (A-6) and (A-3) into (A-8) then simplifying yields

$$\ddot{\underline{r}}_{14} = - \frac{G(M_1 + M_4)}{r_{14}^3} \underline{r}_{14} - GM_2 \left[\frac{\underline{r}_{24}}{r_{24}^3} - \frac{\underline{r}_{21}}{r_{21}^3} \right] - GM_3 \left[\frac{\underline{r}_{34}}{r_{34}^3} - \frac{\underline{r}_{31}}{r_{31}^3} \right] \quad (\text{A-9})$$

As a simplification, arbitrarily let body 2 be the Sun and body 3 the Moon. Also letting $M_1 + M_3 = 1$ where $M_1 = 1 - \mu$, $M_3 = \mu$ and $G = 1$. Then $M_2 = M_s$, and with respect to the other bodies involved $M_4 = 0$. By noting $\underline{r}_{12} = -\underline{r}_{21}$ and $\underline{r}_{13} = -\underline{r}_{31}$ equation (A-9) reduces to

$$\ddot{\underline{r}}_c + \frac{(1-\mu)}{r_c^3} \underline{r}_c = -M_s \left[\frac{\underline{r}_{cs}}{r_{cs}^3} + \frac{\underline{r}_s}{r_s^3} \right] - \mu \left[\frac{\underline{r}_{cm}}{r_{cm}^3} + \frac{\underline{r}_m}{r_m^3} \right] \quad (\text{A-10})$$

where the subscripts c, s and m stand for satellite, Sun and Moon, respectively.

The equations of motion for the Moon are derived in the same manner as the equations of motion for the satellite.

This time the system is solved for $\ddot{\underline{r}}_{13}$; and invoking the

same simplifying assumptions for the satellite gives

$$\ddot{\mathbf{r}}_{13} + \frac{\mathbf{r}_{13}}{r_{13}^3} = -M_S \left[\frac{\mathbf{r}_{23}}{r_{23}^3} + \frac{\mathbf{r}_{12}}{r_{12}^3} \right] \quad (\text{A-11})$$

Lastly, the equations of motion for the Sun are derived using a two-body approximation. Since the Sun is the dominant gravitational body in this model; the combined perturbing effects of the Earth, Moon and satellite upon the Sun are negligible when compared to the reverse effects. In this two-body approximation the masses of the Moon and Earth are assumed to be concentrated at their barycenter. Additionally, the mass of the satellite, with respect to the Sun, Earth and Moon is assumed to be zero. A known solution to this two-body approximation can be shown to be

$$r_s = \frac{P}{1 + e_s \cos v_s} \quad (\text{Ref 9:20}) \quad (\text{A-12})$$

where

$$P = a_s (1 - e_s^2)$$

where a_s is the solar semimajor axis; e_s is the solar eccentricity and v_s is the true anomaly. Equation (A-12) is a polar representation of an elliptic conic section. In terms of Earth-centered non-rotating coordinates the Sun revolves as an unperturbed ellipse with respect to the Earth/Moon barycenter. Rewriting (A-12) into cartesian x/y components with respect to the Earth/Moon barycenter yields

$$X_s = \mu X_m + r_s \cos v_s \quad (\text{A-13})$$

$$Y_s = \mu Y_m + r_s \sin v_s \quad (\text{A-14})$$

where subscripts m refers to the Moon and μ is the distance from the Earth/Moon barycenter to the Earth.

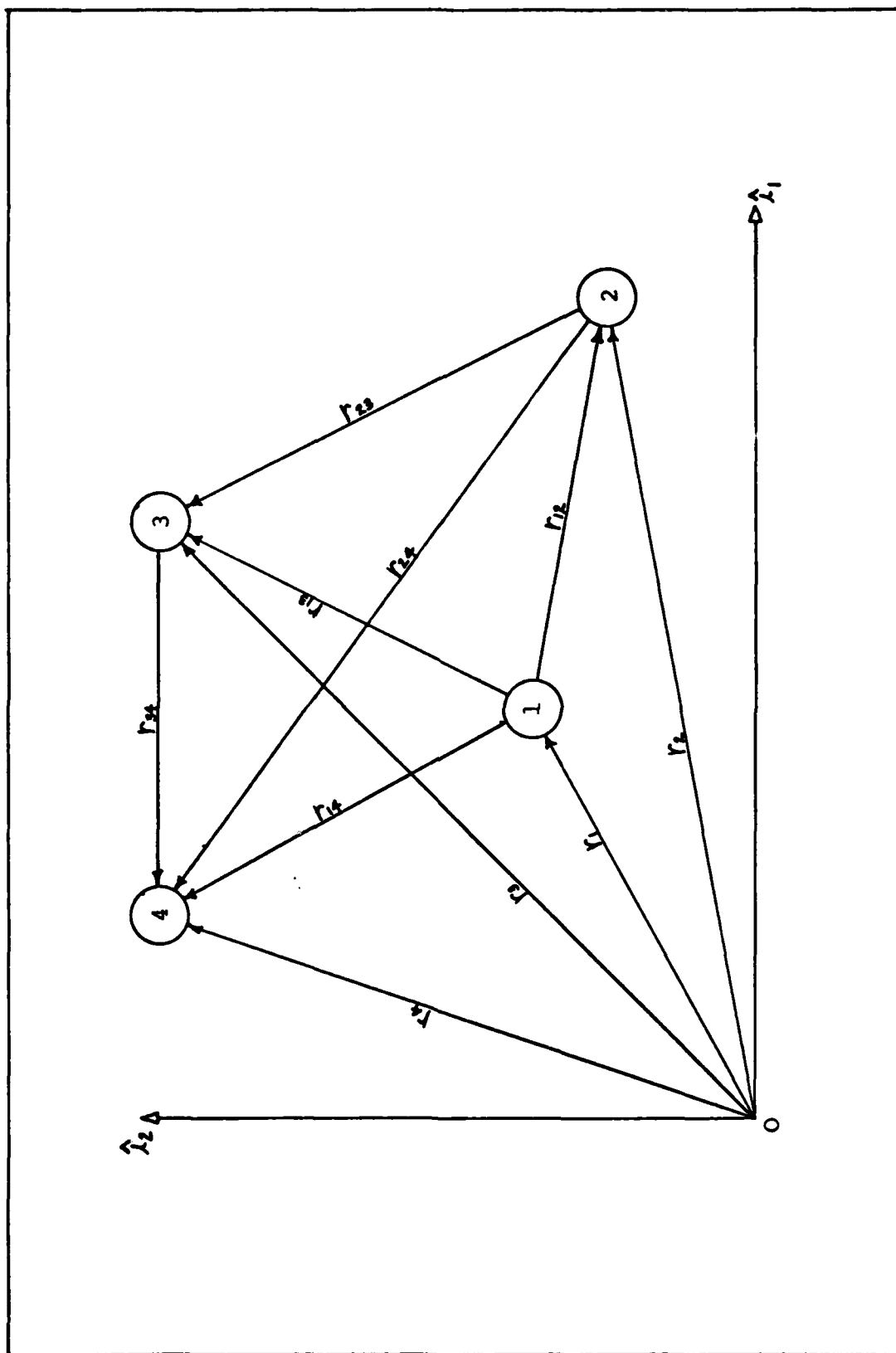


Fig 35. Arbitrary Four-Body System

Vita

Doyne E. Smith was born on September 24, 1945 in Whittier, California. He graduated from Burns Union High School, Burns, Oregon in May of 1963. He enlisted in the United States Air Force in June of 1965. He graduated from Purdue University in May of 1974 with a Bachelor of Science degree in Aeronautical and Astronautical Engineering, and in August of 1974 received a commission in the United States Air Force from Officer Training School. His initial assignment was to Foreign Technology Division, at Wright-Patterson Air Force Base, Ohio. While there, he performed duty as reentry system analyst in the Ballistic Missile Guidance and Reentry Division.

In June of 1978, he was assigned to the Air Force Institute of Technology's resident School of Engineering at Wright-Patterson Air Force Base, Ohio and began his studies toward a Master of Science degree in Astronautical Engineering. After graduation, he will be assigned to Air Defense Command Combat Operations Center in the Cheyenne Mountain Complex, Colorado Springs, Colorado.

Permanent Address: 6865 Vandecar Road
Port Orchard, WN 98366

UNCLASSIFIED

SECURITY CLASSIFICATION OF THIS PAGE (When Data Entered)

REPORT DOCUMENTATION PAGE		READ INSTRUCTIONS BEFORE COMPLETING FORM
1. REPORT NUMBER AFIT/GA/AA/79D-10	2. GOVT ACCESSION NO.	3. RECIPIENT'S CATALOG NUMBER
4. TITLE (and Subtitle) STABILIZING AN UNSTABLE ORBIT ABOUT L_3 IN THE SUN, EARTH, MOON SYSTEM USING LINEAR CONSTANT GAIN FEEDBACK		5. TYPE OF REPORT & PERIOD COVERED MS Thesis
		6. PERFORMING ORG. REPORT NUMBER
7. AUTHOR(s) DOYNE E. SMITH Captain, USAF		8. CONTRACT OR GRANT NUMBER(s)
9. PERFORMING ORGANIZATION NAME AND ADDRESS		10. PROGRAM ELEMENT, PROJECT, TASK AREA & WORK UNIT NUMBERS
11. CONTROLLING OFFICE NAME AND ADDRESS		12. REPORT DATE December, 1979
		13. NUMBER OF PAGES 78
14. MONITORING AGENCY NAME & ADDRESS (if different from Controlling Office)		15. SECURITY CLASS. (of this report) UNCLASSIFIED
		15a. DECLASSIFICATION/DOWNGRADING SCHEDULE
16. DISTRIBUTION STATEMENT (of this Report) Approved for public release; distribution unlimited		
17. DISTRIBUTION STATEMENT (of the abstract entered in Block 20, if different from Report)		
18. SUPPLEMENTARY NOTES Approved for public release; IAW AFR 190-17 Joseph P. Hipps, Maj, USAF Director of Public Affairs A.F.I.T.		
19. KEY WORDS (Continue on reverse side if necessary and identify by block number) Periodic Orbits Libration Points L_3		
20. ABSTRACT (Continue on reverse side if necessary and identify by block number) In this study equations of motion for a satellite in a planar, elliptic four-body system are used to generate an orbit about L_3 . Initial conditions and a periodic reference orbit were found using a circular four-body model. Linear constant gain feedback is used to stabilize the orbit about L_3 in the planar, elliptic four-body model. The computed L_3 orbit is plotted against the reference orbit to assess the effectiveness of position, velocity		

DD FORM 1473

JAN 73

EDITION OF 1 NOV 65 IS OBSOLETE

UNCLASSIFIED

SECURITY CLASSIFICATION OF THIS PAGE (When Data Entered)

UNCLASSIFIED

SECURITY CLASSIFICATION OF THIS PAGE(When Data Entered)

and position/velocity feedback compensation systems. Also computed is the integrated control gain costs for each type of feedback system used. Long term stable motion near libration point L_3 was achieved using position/velocity feedback compensation. Position and velocity feedback when used separately were ineffective as stabilizing feedback compensation systems. The integrated control gain costs also indicate that linear constant gain feedback is not an economical method to stabilize this periodic orbit about L_3 .

SECURITY CLASSIFICATION OF THIS PAGE(When Data Entered)